A POSTERIORI ERROR ESTIMATION FOR THE FINITE ELEMENT METHOD-OF-LINES SOLUTION OF PARABOLIC PROBLEMS

SLIMANE ADJERID†, IVO BABUŠKA‡, AND JOSEPH E. FLAHERTY†

Abstract. Babuška and Yu constructed a posteriori estimates for finite element discretization errors of linear elliptic problems utilizing a dichotomy principal stating that the errors of odd-order approximations arise near element edges as mesh spacing decreases while those of even-order approximations arise in element interiors. We construct similar a posteriori estimates for the spatial errors of finite element method-of-lines solutions of linear parabolic partial differential equations on square-element meshes. Error estimates computed in this manner are proven to be asymptotically correct; thus, they converge in strain energy under mesh refinement at the same rate as the actual errors.

Key Words. Finite element methods, method of lines, a posteriori error estimation, parabolic partial differential equations

AMS (MOS) subject classifications. 65M60, 65M20, 65M15, 65M50

1. Introduction. A posteriori estimates of discretization errors have been an integral part of adaptive finite element methods since their inception nearly twenty years ago [5, 6]. Local contributions to global error estimates furnish *error indicators* that are typically used to control adaptive enrichment through mesh refinement/coarsening (h-refinement) and/or method order variation (p-refinement). Thus, meshes are refined and/or method orders increased where error indicators are large and an opposite course is taken where

† Department of Computer Science and Scientific Computation Research Center, Rensselaer Polytechnic Institute, Troy, NY 12180, USA (adjerids@cs.rpi.edu, flaherje@cs.rpi.edu). This research was partially supported by the U.S. Army Research Office through Contract Number DAAH 04-95-1-0091 and by ARPA/ONR under Grant Number N00014-1779.

‡ Texas Institute for Computational and Applied Mathematics, University of Texas at Austin, Austin, TX 78712.

error indicators are small. An ideal a posteriori error estimation techniques would

i. be *asymptotically correct* in the sense that the error estimate in a particular norm approach zero under enrichment at the same rate as the actual error;

ii. be *computationally simple* by requiring a small fraction of the solution cost;

iii. be *robust* by furnishing accurate estimates for a wide range of meshes and method orders;

iv. provide relatively tight *upper and lower bounds* of the true error in a particular norm; and

v. supply local error indicators that provide global error estimates in *several norms.*

Recent surveys [8, 9, 16] indicate that no error estimates satisfy all of these criteria for all combinations of meshes, method orders, geometries, etc.

Babuška and Yu [10, 18, 19] constructed a posteriori error estimates in strain energy for the finite element solution of linear elliptic problems on square domains by using a dichotomy principal stating that the errors of odd-order approximations arise at element edges as the spacing of a square-element mesh decreases to zero while those of even-order approximations arise in element interiors in the same limit. Yu [18, 19] established the asymptotic correctness of these error estimates for finite element spaces consisting of piecewise bi-polynomials of arbitrary degree. Adjerid et al. [3] showed that similar estimates could be obtained for the spatial discretization errors of method-of-lines solutions of one-dimensional parabolic partial differential equations. We extend this earlier work by constructing a posteriori estimates for the spatial errors of finite element method-of-lines solutions of two-dimensional linear parabolic equations. We establish asymptotic correctness of these error estimates on square elements and show that temporal variations of spatial errors may be neglected for both odd- (§3) and even-order (§4.2) finite element solutions. Error estimates of even-order finite element solutions may also be obtained by

solving local parabolic problems (§4.1), which include the temporal variation of the error estimate. This procedure might be useful when error estimates are used to control mesh motion (r-refinement) [2].

Both odd- and even-order error estimation procedures are computationally simple. The odd-order estimates only require jumps in solution gradients at the four element vertices and neither element nor edge residuals are needed. Only nearest-neighbor interaction is necessary; thus, simplifying implementation on a parallel computer. Gradient jumps may be shared between elements sharing a vertex to halve the cost relative to element-by-element computation. The even-order elliptic and parabolic estimates are local to the element. No off-element communication is necessary; hence, there is no search for neighbor information and parallelization is perfect. Computations (§5) imply that the even-order estimates improve with increasing polynomial degree.

Numerical examples presented in §5 and elsewhere [1] indicate that the error estimates are applicable more widely than the present theory would suggest. Thus, for example, they appear to work in the presence of some nonlinearity, when some singularities are present, and on graded quadrilateral-element meshes. Experiments of Baehmann et al. [4] and Ilin et al. [11] would suggest that the even-order estimates are applicable to triangular elements.

2. Formulation. Consider the linear, scalar, two-dimensional parabolic differential equation

$$\partial_t u + \mathbf{L}u = f(\mathbf{x}), \quad \mathbf{x} = [x_1, x_2]^T \in \Omega, \quad t > 0, \tag{2.1a}$$

with

$$\mathbf{L}u = -\sum_{j=1}^{2}\sum_{k=1}^{2} \partial_{x_j}(a_{j,k}(\mathbf{x})\partial_{x_k} u) + b(\mathbf{x})u, \tag{2.1b}$$

on a bounded rectangle Ω subject to the initial and Dirichlet boundary conditions

$$u(\mathbf{x},0) = u^0(\mathbf{x}), \quad \mathbf{x} \in \Omega \cup \partial\Omega, \tag{2.1c}$$

$$u(\mathbf{x},t) = 0, \quad \mathbf{x} \in \partial\Omega, \quad t \geq 0. \tag{2.1d}$$

The functions $a_{j,k}(\mathbf{x})$, $j, k = 1, 2$, and $b(\mathbf{x})$ are smooth with $\mathbf{L}$ being a positive-definite operator.

The Galerkin form of (2.1) consists of determining $u \in H_0^1$ satisfying

$$(v,\partial_t u) + A(v,u) = (v,f), \quad t > 0, \tag{2.2a}$$

$$A(v,u) = A(v,u^0), \quad t = 0, \quad \text{for } all \ v \in H_0^1, \tag{2.2b}$$

where the strain energy and L^2 inner products, respectively, are

$$A(v,u) = \iint_\Omega [\sum_{j=1}^{2} \sum_{k=1}^{2} a_{j,k}(\mathbf{x}) \partial_{x_j} v \, \partial_{x_k} u + b(\mathbf{x}) vu] \, dx_1 dx_2 \tag{2.2c}$$

and

$$(v,u) = (v,u)_0 = \iint_\Omega uv \, dx_1 dx_2. \tag{2.2d}$$

As usual, functions in the Sobolev space H^s, $s \geq 0$, have the inner product and norm

$$(v,u)_s = \sum_{|\alpha| \leq s} (\partial_{x_1}^{\alpha_1} \partial_{x_2}^{\alpha_2} v, \partial_{x_1}^{\alpha_1} \partial_{x_2}^{\alpha_2} u), \quad \|u\|_1^2 = (u,u)_s, \tag{2.2e,f}$$

where $|\alpha| = \alpha_1 + \alpha_2$. The subscript 0 on H^1 additionally restricts functions to satisfy (2.1d).

Finite element solutions of (2.2a,b) are obtained by approximating H^1 by a finite-dimensional subspace $S^{N,p}$ and determining $U \in S_0^{N,p}$ such that

$$(V,\partial_t U) + A(V,U) = (V,f), \quad t > 0, \tag{2.3a}$$

$$A(V,U) = A(V,u^0), \quad t = 0, \quad \text{for } all \ V \in S_0^{N,p}. \tag{2.3b}$$

Partitioning Ω into a uniform mesh of square elements Δ_i, $i = 1, 2, \cdots, N$, define $S^{N,p}$ as

$$S^{N,p} = \{ w \in H^1 \mid w(\mathbf{x}) \in Q_p(\Delta_i), \mathbf{x} \in \Delta_i, i = 1, 2, \cdots, N \} \tag{2.4}$$

where $Q_p(\Delta_i)$ is the space of bi-polynomial functions that are products of univariate polynomials of degree p in x_1 and x_2 on Δ_i.

The following two lemmas describe standard interpolation and a priori discretization error estimates for finite element solutions of (2.2) that will be useful during the subsequent analysis.

LEMMA 2.1. *Let* $W \in S_0^{N,p}$ *be an interpolant of* $w \in H_0^1 \cap H^{p+1}$ *that is exact when* $w \in Q_p(\Omega)$. *Then, there exists a constant* $C > 0$ *such that*

$$\|W - w\|_s \leq Ch^{p+1-s}\|w\|_{p+1}, \quad s = 0, 1, \tag{2.5a}$$

where

$$h = 1/\sqrt{N}. \tag{2.5b}$$

Proof. Cf., e.g., Oden and Carey [12]. □

LEMMA 2.2. *Let* u *and* U *be solutions of (2.2a,b) and (2.3), respectively. Further let*

$$A(V,\hat{U}) = A(V,u), \quad \text{for all } V \in S_0^{N,p}, \quad t \geq 0, \tag{2.6}$$

be the strain energy projection of u onto $S_0^{N,p}$. *If* $u^0 \in H_0^1 \cap H^2$ *and* u *is smooth enough for all terms in (2.7) to be bounded, then there exist* $C > 0$ *and* $t_0 > 0$ *such that*

$$\|\hat{U} - U\|_1^2 \leq Ch^{2(p+1)} \int_0^t \|\partial_t u(\cdot,\tau)\|_{p+1}^2 \, d\tau, \quad t \geq 0, \tag{2.7a}$$

$$\|\partial_t^n e(\cdot,t)\|_0 \leq Ch^{p+1}\left[\|u^0\|_2 + \sum_{l=0}^{n} \|\partial_t^l u(\cdot,t)\|_{p+1} + \int_{t-t_0}^{t} \|\partial_t^{n+1} u(\cdot,\tau)\|_{p+1} \, d\tau\right.$$

$$\left. + \int_0^t \|\partial_t u(\cdot,\tau)\|_2 \, d\tau\right], \quad t > t_0 > 0, \quad n \geq 0, \tag{2.7b}$$

$$\|\partial_t^n e(\cdot,t)\|_1 \leq Ch^p\left[\|u^0\|_2 + \sum_{l=0}^{n} \max_{t-t_0<\tau<t} \|\partial_t^l u(\cdot,\tau)\|_{p+1} + \left[\int_{t-t_0}^{t} \|\partial_t^{n+1} u(\cdot,\tau)\|_p^2 \, d\tau\right]^{1/2}\right.$$

$$\left. + h\|u^0\|_0 + h\int_0^t \|f\|_0 \, d\tau\right], \quad t > t_0 > 0, \quad n \geq 0, \tag{2.7c}$$

where

$$e(\mathbf{x},t) = u(\mathbf{x},t) - U(\mathbf{x},t). \tag{2.7d}$$

Proof. Cf. Wait and Mitchell [17], e.g., for the proof of (2.7a) and Thomée [15] for the proofs of (2.7b) and (2.7c). □

2.1. Preliminary considerations. Let $\tilde{\pi}[\bar{z}]$ be the univariate operator that interpolates functions in $H_0^1(\bar{z}-h/2,\bar{z}+h/2)$ at the Lobatto points of degree $p+1$, $p \geq 1$, on $[\bar{z}-h/2,\bar{z}+h/2]$. Also let

$$\psi_{p+1}(\bar{z},z) = z^{p+1} - \tilde{\pi}[\bar{z}]z^{p+1} \tag{2.8}$$

vanish at these $p+1$ Lobatto points. Hence, $\psi_{p+1}(\bar{z},z)$ and $\psi'_{p+1}(\bar{z},z)$ are, respectively, proportional to Lobatto and Legendre polynomials on $[\bar{z}-h/2,\bar{z}+h/2]$, with $(\,)'$ denoting ordinary differentiation.

We use $\tilde{\pi}$ to define a two-dimensional interpolation operator π_i on element i satisfying $\pi_i u(\mathbf{x}) = \tilde{\pi}[\bar{x}_{1,i}]\tilde{\pi}[\bar{x}_{2,i}]u(\mathbf{x}) \in Q_p(\Delta_i)$, $\mathbf{x} \in \Delta_i$. Since the mesh is uniform, we will omit the elemental index i and the dependence of $\tilde{\pi}[\bar{x}_{j,i}]$ and $\psi(\bar{x}_{j,i},x_i)$ on the coordinates of the cell center $(\bar{x}_{1,i},\bar{x}_{2,i})$, $i = 1, 2, \cdots, N$, whenever confusion is unlikely.

The functions $\psi_{p+1}(x_j)$, $j = 1, 2$, provide the dominant contributions to the spatial discretization error on element Δ for both odd- and even-order finite element approximations. Indeed, we shall show that estimates $E(\mathbf{x},t)$ of $e(\mathbf{x},t)$ have the form

$$E(\mathbf{x},t) = b_1(t)\psi_{p+1}(x_1) + b_2(t)\psi_{p+1}(x_2), \quad \mathbf{x} \in \Delta. \tag{2.9}$$

The following sequence of lemmas take steps in this direction.

LEMMA 2.3. *Let* $u \in H^{p+2}$, $t \geq 0$, *then*

$$u(\mathbf{x},t) - \pi u(\mathbf{x},t) = \phi(\mathbf{x},t) + \gamma(\mathbf{x},t), \quad \mathbf{x} \in \Delta, \tag{2.10a}$$

where

$$\phi(\mathbf{x},t) = \beta_1(t)\psi_{p+1}(x_1) + \beta_2(t)\psi_{p+1}(x_2), \tag{2.10b}$$

$$\|\partial_t^n \phi\|_{s,\Delta} \leq Ch^{p+1-s}\|\partial_t^n u\|_{p+1,\Delta}, \quad t \geq 0, \quad n \geq 0, \quad s = 0, 1, \cdots, p, \tag{2.10c}$$

$$\|\partial_{x_j}\phi\|_{0,\Delta} \le Ch^p \|u\|_{p+1,\Delta}, \quad j = 1,2, \quad t \ge 0, \tag{2.10d}$$

$$\|\gamma\|_{s,\Delta} \le Ch^{p+2-s} \|u\|_{p+2,\Delta}, \quad s = 0, 1, \cdots, p+1, \tag{2.10e}$$

and

$$\|\partial_{x_j}\gamma\|_{s,\Delta} \le Ch^{p+1-s} \|u\|_{p+2,\Delta}, \quad s = 0, 1, \quad j = 1, 2, \quad t \ge 0. \tag{2.10f}$$

Remark. Local Sobolev norms are defined like their global counterparts (2.2d,e) with Ω replaced by Δ.

Proof. Yu's [18] results for elliptic partial differential equations extend directly to the transient case. □

LEMMA 2.4. *Let* $\Pi u \in S_0^{N,p}$ *be an interpolant of* $u \in H^{p+2}$ *for* $\mathbf{x} \in \Omega$ *that agrees with* πu *when* $\mathbf{x} \in \Delta$, *then*

$$|A(W, u - \Pi u)| \le Ch^{p+1} \|u\|_{p+2} \|W\|_1, \quad \text{for all } W(\mathbf{x}) \in S_0^{N,p}. \tag{2.11}$$

Proof. cf. Yu [18]. □

LEMMA 2.5. *Let* $u \in H_0^1 \cap H^{p+2}$, $U \in S_0^{N,p}$, *and* $\hat{U} \in S_0^{N,p}$, *be solutions of (2.2a,b), (2.3), and (2.6), respectively. Further let* $\Pi u \in S_0^{N,p}$ *interpolate* u *as described in Lemma 2.4, then*

$$\|\hat{U} - \Pi u\|_1 \le Ch^{p+1} \|u\|_{p+2}, \quad \|U - \Pi u\|_1 \le C(u) h^{p+1}, \tag{2.12a,b}$$

and

$$e(\mathbf{x},t) = \Phi(\mathbf{x},t) + \Theta(\mathbf{x},t) \tag{2.13a}$$

where the restrictions of $\Phi(\mathbf{x},t)$ *and* $\Theta(\mathbf{x},t)$ *to* Δ *are* $\phi(\mathbf{x},t)$ *of (2.10b) and*

$$\theta(\mathbf{x},t) = \gamma(\mathbf{x},t) + \pi u(\mathbf{x},t) - U(\mathbf{x},t). \tag{2.13b}$$

Furthermore,

$$\|\nabla\Phi\|_0^2 \le Ch^{2p} \|u\|_{p+1}^2, \quad \|\nabla\Theta\|_0^2 \le C(u) h^{2(p+1)}, \tag{2.13c,d}$$

and

$$\|\partial_t^n \Theta\|_s \le C(u) h^{p+1-s}, \quad n \ge 0, \quad s = 0, 1, \quad t > t_0. \tag{2.13e}$$

Proof. Subtract $A(V,\Pi u)$ from (2.6) and use (2.11) to obtain

$$|A(V,\hat{U}-\Pi u)| = |A(V,u-\Pi u)| \le Ch^{p+1}\|u\|_{p+2}\|V\|_1, \quad \text{for all } V \in S_0^{N,p}. \tag{2.14}$$

Replacing V in (2.14) by $\hat{U} - \Pi u$ yields (2.12a). Addition and subtraction of $\hat{U}$ to $U - \Pi u$ and subsequent use of the triangular inequality with (2.7a) and (2.12a) establishes (2.12b).

In order to prove (2.13c-e), use (2.10a) and (2.13b) to obtain

$$e = u - \pi u + \pi u - U = \phi + \gamma + \pi u - U = \phi + \theta, \quad \mathbf{x} \in \Delta, \tag{2.15}$$

and, consequently, (2.13a). Squaring and summing (2.10d) over the elements of the mesh leads to (2.13c). Taking the gradient and L^2 norm of (2.13b) and using the triangular inequality yields

$$\|\nabla\theta\|_{0,\Delta}^2 \le C(\|\nabla\gamma\|_{0,\Delta}^2 + \|\nabla(\pi u - U)\|_{0,\Delta}^2) \tag{2.16}$$

The use of (2.10f) and (2.12b) with a summation over all elements yields (2.13d). In a similar manner, a combination of (2.13a), (2.7b,c), and (2.10c) yields (2.13e). □

LEMMA 2.6. *Under the conditions of Lemma 2.5, there exists a function* ε_1 *such that*

$$\|e\|_1^2 = \|u - \Pi u\|_1^2 + \varepsilon_1 \tag{2.17a}$$

with

$$|\varepsilon_1| \le C(u)h^{2p+1}. \tag{2.17b}$$

Proof. Adding and subtracting Πu to e yields (2.17a) with

$$\varepsilon_1 = 2(u - \Pi u, \Pi u - U)_1 + \|\Pi u - U\|_1^2. \tag{2.18}$$

Applying the Schwarz inequality and using (2.5) and (2.12b) yields (2.17b). □

3. A posteriori error estimation of odd-degree approximations. If u is smooth on Δ then error estimates $E(\mathbf{x},t)$ of odd-degree approximations may be constructed in terms of jumps in derivatives of U at the vertices of Δ. Informally, use (2.7d) to and its approximation (2.9) to compute jumps in the derivatives of $e(\mathbf{x},t)$ at the vertices $\mathbf{p}_k = (p_{1k},p_{2k})$,

$k = 1, 2, 3, 4$, of Δ as

$$[\partial_{x_j} e(\mathbf{p}_k,t)]_j = -[\partial_{x_j} U(\mathbf{p}_k,t)]_j \approx b_1(t)[\partial_{x_j}\psi_{p+1}(p_{1k})]_j + b_2(t)[\partial_{x_j}\psi_{p+1}(p_{2k})]_j,$$

$$j = 1, 2, \quad k = 1, 2, 3, 4, \quad \mathbf{x} \in \Delta, \tag{3.1}$$

where $[q(\mathbf{p})]_j$ denotes the jump in q at point $\mathbf{p}$ in the x_j direction. Since jumps in the solution U and ψ_{p+1} are known, this overdetermined system may be solved in some sense for the coefficients b_j, $j = 1, 2$. The procedure used in the following lemma and theorem is to solve (3.1) for b_j, $j = 1, 2$, at each element vertex $\mathbf{p}_k$, $k = 1, 2, 3, 4$, and average the values of $\|E(\cdot,t)\|_{1,\Delta}$ based on the pairs of b_j, $j = 1, 2$, obtained.

LEMMA 3.1. *Let $u \in H_0^1 \cap H^{p+2}$, Πu be as defined in Lemma 2.4, and p be a positive odd integer, then*

$$\|u - \Pi u\|_1^2 = \frac{h^2}{16(2p+1)} \sum_{i=1}^{N} \sum_{j=1}^{2} \sum_{k=1}^{4} [\partial_{x_j} \Pi u(\mathbf{p}_k,t)]_j^2 + \varepsilon_2 \tag{3.2a}$$

where

$$|\varepsilon_2| \le Ch^{2p+1}, \tag{3.2b}$$

Proof. cf. Yu [19]. □

THEOREM 3.1. *Let $u \in H_0^1 \cap H^{p+2}$ and $U \in S_0^{N,p}$ be solutions of (2.2) and (2.3), respectively. If p is an odd positive integer, then*

$$\|e(\cdot,t)\|_1^2 = \|E(\cdot,t)\|_1^2 + \varepsilon \tag{3.3a}$$

where

$$\|E(\cdot,t)\|_1^2 = \frac{h^2}{16(2p+1)} \sum_{i=1}^{N} \sum_{j=1}^{2} \sum_{k=1}^{4} [\partial_{x_j} U(\mathbf{p}_k,t)]_j^2, \quad |\varepsilon| \le Ch^{2p+1}. \tag{3.3b,c}$$

Proof. Adding and subtracting Πu on each element yields

$$\frac{h^2}{16(2p+1)} \sum_{i=1}^{N} \sum_{j=1}^{2} \sum_{k=1}^{4} [\partial_{x_j} U(\mathbf{p}_k,t)]_j^2 = \frac{h^2}{16(2p+1)} \sum_{i=1}^{N} \sum_{j=1}^{2} \sum_{k=1}^{4} [\partial_{x_j} \Pi u(\mathbf{p}_k,t)]_j^2 + \varepsilon_3 \tag{3.4a}$$

where

$$\varepsilon_3 = \frac{h^2}{16(2p+1)} \sum_{i=1}^{N} \sum_{j=1}^{2} \sum_{k=1}^{4} \{[\partial_{x_j}(U(\mathbf{p}_k,t) - \Pi u(\mathbf{p}_k,t))]_j^2 +$$

$$2[\partial_{x_j}(U(\mathbf{p}_k,t) - \Pi u(\mathbf{p}_k,t))]_j [\partial_{x_j} \Pi u(\mathbf{p}_k,t)]_j \}. \tag{3.4b}$$

Using (3.2a) and (2.17a) in (3.4a) we obtain

$$\frac{h^2}{16(2p+1)} \sum_{i=1}^{N} \sum_{j=1}^{2} \sum_{k=1}^{4} [\partial_{x_j} U(\mathbf{p}_k,t)]_j^2 = \|e\|_1^2 - \varepsilon_1 - \varepsilon_2 + \varepsilon_3; \tag{3.4c}$$

thus, establishing (3.3a,b) with $\varepsilon = \varepsilon_1 + \varepsilon_2 - \varepsilon_3$. Since ε_1 and ε_2 are $O(h^{2p+1})$, it remains to find a similar bound for ε_3. To this end, an application of the Schwarz inequality to (3.4b) yields

$$|\varepsilon_3| \le \frac{h^2}{16(2p+1)} \sum_{i=1}^{N} \sum_{j=1}^{2} \sum_{k=1}^{4} [\partial_{x_j}(U(\mathbf{p}_k,t) - \Pi u(\mathbf{p}_k,t))]_j^2 +$$

$$2\{\frac{h^2}{16(2p+1)} \sum_{i=1}^{N} \sum_{j=1}^{2} \sum_{k=1}^{4} [\partial_{x_j}(U(\mathbf{p}_k,t) - \Pi u(\mathbf{p}_k,t))]_j^2\}^{1/2} \times$$

$$\{\frac{h^2}{16(2p+1)} \sum_{i=1}^{N} \sum_{j=1}^{2} \sum_{k=1}^{4} [\partial_{x_j} \Pi u(\mathbf{p}_k,t)]_j^2\}^{1/2}. \tag{3.5}$$

Let Δ_0 be the canonical element $-1 \le \xi_1,\xi_2 \le 1$ and use norm equivalence on the finite-dimensional space $Q_p(\Delta_0)$ to show that

$$\max_{(\xi_1,\xi_2)\in\Delta_0} (|\partial_{\xi_1} v| + |\partial_{\xi_2} v|) \le C \|\nabla v\|_{0,\Delta_0}, \quad \text{for } all \ v \in Q_p(\Delta_0). \tag{3.6a}$$

A subsequent linear mapping of Δ_0 to an element Δ_i, $i = 1, 2, \cdots, N$, yields

$$\max_{(x_1,x_2)\in\Delta_i} (|\partial_{x_1} w| + |\partial_{x_2} w|) \le \frac{C}{h} \|w\|_{1,\Delta_i}, \quad \text{for } all \ w \in Q_p(\Delta_i). \tag{3.6b}$$

Let $\Delta_{i,n}$, $n = 1, 2, 3, 4$, denote the four elements having common edges with $\Delta_{i,0} = \Delta_i$ and

$$\Delta_i^* = \bigcup_{n=0}^{4} \Delta_{i,n}. \tag{3.7}$$

Then, using (3.6b),

$$[\partial_{x_j}(U(\mathbf{p}_k,t) - \Pi u(\mathbf{p}_k,t))]_j \le C \max_{(x_1,x_2)\in\Delta_i^*} \{|\partial_{x_1}(U - \Pi u)| + |\partial_{x_2}(U - \Pi u)| \le$$

$$\frac{C}{h}\|U - \Pi u\|_{1,\Delta_i^*}, \quad j = 1, 2, \quad k = 1, 2, 3, 4. \tag{3.8}$$

With (3.8), we have

$$\frac{h^2}{16(2p+1)} \sum_{i=1}^{N} \sum_{j=1}^{2} \sum_{k=1}^{4} [\partial_{x_j}(U(\mathbf{p}_k,t) - \Pi u(\mathbf{p}_k,t))]_j^2 \le$$

$$\frac{C}{16(2p+1)} \sum_{i=1}^{N} \|U - \Pi u\|_{1,\Delta_i^*}^2 \le C\|U - \Pi u\|_1^2. \tag{3.9a}$$

Similarly, using (2.5) and (3.2), we have

$$\frac{h^2}{16(2p+1)} \sum_{i=1}^{N} \sum_{j=1}^{2} \sum_{k=1}^{4} [\partial_{x_j}\Pi u(\mathbf{p}_k,t)]_j^2 \le C\|u - \Pi u\|_1^2. \tag{3.9b}$$

Using (3.9) in (3.5) yields

$$|\varepsilon_3| \le C\{\|U - \Pi u\|_1^2 + \|u - \Pi u\|_1 \|U - \Pi u\|_1\}. \tag{3.10}$$

The estimates (2.5) and (2.12b) imply that $\varepsilon_3 = O(h^{2p+1})$, which completes the proof. □

4. A posteriori error estimation of even-degree approximations. Error estimates in terms of jumps in solution derivatives fail for even-order approximations since $\psi_{p+1}(x_j)$, $j = 1, 2$, is continuous on $\partial\Delta$. Thus, with p even, we construct a Galerkin problem for e by replacing u in (2.2) by $U + e$ to obtain

$$(v,\partial_t e) + A(v,e) = g(t,v), \quad t > 0, \tag{4.1a}$$

$$A(v,e) = A(v,u^0 - U), \quad t = 0, \quad \text{for } all \ v \in H_0^1, \tag{4.1b}$$

with

$$g(t,v) = (v,f) - (v,\partial_t U) - A(v,U). \tag{4.1c}$$

The error is once again approximated by E according to (2.9) and the test function v is

selected as

$$v_j(\mathbf{x}) = (x_j - \bar{x}_{j,i})\delta(x_1)\delta(x_2), \quad j = 1, 2, \tag{4.2a}$$

where

$$\delta(z) = \frac{\psi_{p+1}(z)}{z - \bar{z}}, \quad \sigma(z) = \psi'_{p+1}(z), \quad z \in [\bar{z}-h/2,\bar{z}+h/2]. \tag{4.2b,c}$$

(Although not yet needed, we define σ for future reference.) Since $\psi_{p+1}(x_j)$ and $v_j(\mathbf{x})$, $j = 1, 2$, vanish on $\partial\Delta_i$, the error estimate satisfies the local Dirichlet problems

$$(v_j,\partial_t E)_\Delta + A_\Delta(v_j,E) = g_\Delta(t,v_j), \quad t > 0 \tag{4.3a}$$

$$A_\Delta(v_j,E) = A_\Delta(v_j,u^0 - U), \quad t = 0, \quad j = 1, 2. \tag{4.3b}$$

where Δ subscripts denote that inner products are restricted to Δ_i. The time derivative of E in (4.3a) may be neglected to obtain the local elliptic problem

$$A_\Delta(v_j,E) = g_\Delta(t,v_j), \quad t > 0, \quad j = 1, 2. \tag{4.4}$$

The parabolic (4.3) and elliptic (4.4) error estimates are shown to be asymptotically correct in §4.1 and §4.2, respectively; however, prior to this, we establish some properties of ψ_{p+1}, δ, σ, and v_j, $j = 1, 2$.

LEMMA 4.1. *Let $p \geq 2$ be an even integer, then there exist $C > 0$ such that*

$$\iint_\Delta \delta(x_j)\,dx_1dx_2 = Ch^{p+2}, \quad \iint_\Delta \psi_{p+1}(x_j)^2\delta(x_k)\,dx_1dx_2 = Ch^{3p+4}, \tag{4.5a,b}$$

$$\iint_\Delta \sigma(x_j)^2\delta(x_k)\,dx_1dx_2 = Ch^{3p+2}, \quad \|\sigma(x_j)\|^2_{0,\Delta} = Ch^{2(p+1)}, \tag{4.5c,d}$$

$$ch^{2(p-s)+4} \leq \|\psi_{p+1}(x_j)\|^2_{s,\Delta} \leq Ch^{2(p-s)+4}, \quad s = 0, 1, \tag{4.5e}$$

$$ch^{2p+1} \leq \|v_j(\cdot)\|_{1,\Delta} \leq Ch^{2p+1}, \quad j, k = 1, 2. \tag{4.5f}$$

Proof. A direct computation reveals the results. □

4.1. The parabolic error estimate. The parabolic finite element problem (4.3) may

be further simplified by neglecting the higher-order off-diagonal diffusion coefficients and the reaction term in the strain energy (2.2c), freezing the diagonal diffusion coefficients, and using symmetry properties of $\psi_{p+1}(z)$ and $v_j(\mathbf{x})$, $j = 1, 2$, to obtain the uncoupled constant-coefficient initial value problem on element i

$$b'_j(t) + r_j b_j(t) = G_j(t), \quad t > 0, \tag{4.6a}$$

$$b_j(0) = \frac{A_\Delta(v_j, u^0(\cdot) - U(\cdot,0))}{\bar{a}_{j,j} \iint_\Delta \sigma^2(x_j)\delta(x_{(j \bmod 2)+1})\, dx_1 dx_2}, \quad j = 1, 2, \tag{4.6b}$$

where

$$r_j = \bar{a}_{j,j} \frac{\iint_\Delta \sigma^2(x_j)\delta(x_{(j \bmod 2)+1})\, dx_1 dx_2}{\iint_\Delta \psi_{p+1}^2(x_j)\delta(x_{(j \bmod 2)+1})\, dx_1 dx_2}, \tag{4.6c}$$

$$G_j(t) = \frac{g_\Delta(t, v_j)}{\iint_\Delta \psi_{p+1}^2(x_j)\delta(x_{(j \bmod 2)+1})\, dx_1 dx_2}, \tag{4.6d}$$

and

$$\bar{a}_{jk} = a_{jk}(\bar{\mathbf{x}}), \quad j, k = 1, 2. \tag{4.6e}$$

Of course, the exact solution of (4.6) is

$$b_j(t) = b_j(0)e^{-r_j t} + \int_0^t e^{-r_j(t-\tau)} G_j(\tau)\, d\tau, \quad t \geq 0, \quad j = 1, 2. \tag{4.7}$$

In order to estimate the difference between the exact solution of (4.1) and its approximation by (2.9, 4.7), we substitute (2.13) into (4.1) while using (2.10b) to obtain

$$\beta'_j(t) + r_j \beta_j(t) = G_j(t) - F_j(t) - H_j(t), \quad t > 0, \tag{4.8a}$$

$$\beta_j(0) = \frac{A_\Delta(v_j, u^0(\cdot) - U(\cdot,0))}{\bar{a}_{j,j} \iint_\Delta \sigma^2(x_j)\delta(x_{(j \bmod 2)+1})\, dx_1 dx_2} - \frac{F_j(0)}{r_j}, \tag{4.8b}$$

where

$$F_j(t) = \frac{\iint_\Delta [\sum_{k=1}^{2}\sum_{l=1}^{2} a_{k,l}\partial_{x_k} v_j \partial_{x_l}\theta + \sum_{k=1}^{2}\sum_{l=1}^{2}(a_{k,l}-\bar{a}_{k,l})\partial_{x_k} v_j \partial_{x_l}\phi + bv_j e]\, dx_1 dx_2}{\iint_\Delta \psi_{p+1}^2(x_j)\delta(x_{(j \bmod 2)+1})\, dx_1 dx_2}, \quad j = 1, 2, \tag{4.8c}$$

$$H_j(t) = \frac{(v_j, \partial_t \theta)}{\iint_\Delta \psi_{p+1}^2(x_j)\delta(x_{(j \bmod 2)+1})\, dx_1 dx_2}, \quad j = 1, 2. \tag{4.8d}$$

We may formally solve (4.8a) for β_j to obtain

$$\beta_j(t) = \beta_j(0)e^{-r_j t} + \int_0^t e^{-r_j(t-\tau)}[G_j(\tau) - F_j(\tau) - H_j(\tau)]\, d\tau, \quad t \geq 0, \quad j = 1, 2. \tag{4.9}$$

The following Lemma quantifies the differences between β_j and its approximation b_j, $j = 1, 2$.

LEMMA 4.2. *Let* $p \geq 2$ *be an even integer,* $u \in H_0^1 \cap H^{p+2}$, $t \geq 0$, *and* $a_{k,k}(\mathbf{x}) > \alpha_0 > 0$, $\mathbf{x} \in \Omega$, $k = 1, 2$, *and assume that*

$$\|\partial_t^n e\|_1 \leq C(u), \quad n = 0, 1, \quad 0 \leq t \leq t_0, \tag{4.10}$$

Then,

$$\sum_{i=1}^{N}(\beta_{ji} - b_{ji})^2 \leq C(u), \quad \sum_{i=1}^{N}(\beta_{ji}^2 - b_{ji}^2) \leq \frac{C(u)}{h}, \quad j = 1, 2, \quad t > t_0. \tag{4.11a,b}$$

Proof. Letting

$$\alpha_j(t) = \beta_j(t) - b_j(t), \quad j = 1, 2, \tag{4.12}$$

and subtracting (4.7) from (4.9) and (4.6b) from (4.8b) we obtain

$$\alpha_j(t) = \alpha_j(0)e^{-r_j t} - \int_0^t e^{-r_j(t-\tau)}[F_j(\tau) + H_j(\tau)]\, d\tau, \quad t \geq 0, \tag{4.13a}$$

with

$$\alpha_j(0) = -\frac{F_j(0)}{r_j}, \quad j = 1, 2. \tag{4.13b}$$

Integrating (4.13a) by parts and applying the Schwarz and triangular inequalities yields

$$\alpha_j^2(t) \le C[e^{-2r_j t}\alpha_j^2(0) + \frac{|F_j(t) + H_j(t)|^2}{r_j^2} + e^{-2r_j t}\frac{|F_j(0) + H_j(0)|^2}{r_j^2} +$$

$$e^{-2r_j(t-t_0)}\int_0^{t_0} \frac{|F_j'(\tau) + H_j'(\tau)|^2}{r_j^3}\,d\tau + \int_{t_0}^{t} \frac{|F_j'(\tau) + H_j'(\tau)|^2}{r_j^3}\,d\tau], \quad t \ge 0. \tag{4.14}$$

It remains to bound the various terms in (4.14). To begin, apply the Schwarz and triangular inequalities to (4.8c) while using the assumed smoothness of the coefficients $a_{k,l}$, $k, l = 1, 2$, and the dominance of the H^1 norm relative to the L^2 norm to obtain

$$|F_j(t) + H_j(t)|^2 \le C\frac{\|v_j\|_{1,\Delta}^2[\|\theta\|_{1,\Delta}^2 + h^2\|\phi\|_{1,\Delta}^2 + \|e\|_{0,\Delta}^2 + \|\theta_t\|_{0,\Delta}^2]}{[\iint_\Delta \psi_{p+1}^2(x_j)\delta(x_{(j \bmod 2)+1})\,dx_1 dx_2]^2}, \quad j = 1, 2. \tag{4.15}$$

A summation over the elements and use of (4.6c) and (4.5) reveals that

$$\sum_{i=1}^{N} \frac{|F_{ji}(t) + H_{ji}(t)|^2}{r_{ji}^s} \le Ch^{2(s-p-3)}[\|\Theta\|_1^2 + h^2\|\Phi\|_1^2 + \|e\|_0^2 + \|\partial_t\Theta\|_0^2],$$

$$j = 1, 2, \quad s \ge 0, \quad t \ge 0. \tag{4.16}$$

The terms on the right may be bounded for $t > t_0$ using (2.7b) and (2.13). Additionally, since $\|e\|_0$ is bounded on $0 \le t < t_0$, (4.16) may be written as

$$\sum_{i=1}^{N} \frac{|F_{ji}(t) + H_{ji}(t)|^2}{r_{ji}^s} \le \begin{cases} C(u)h^{2(s-p-3)}, & \text{if } 0 \le t < t_0 \\ C(u)h^{2(s-2)}, & \text{if } t_0 < t \end{cases}, \quad j = 1, 2, \quad s \ge 0. \tag{4.17}$$

In a similar manner,

$$\sum_{i=1}^{N} \frac{|F_j'(t) + H_j'(t)|^2}{r_j^3} \le \begin{cases} C(u)h^{-2p}, & \text{if } 0 \le t \le t_0 \\ C(u), & \text{if } t_0 < t \end{cases}, \quad j = 1, 2. \tag{4.18}$$

The initial data $\alpha_j(0)$, $j = 1, 2$, may be bounded by applying the Schwarz inequality to (4.13b) and using (4.5) to obtain

$$\alpha_j(0)^2 \le Ch^{-2(p+1)}[\|\theta(\cdot,0)\|^2_{1,\Delta} + h^2\phi(\cdot,0)\|^2_{1,\Delta} + \|e(\cdot,0)\|^2_{0,\Delta}], \quad j = 1, 2. \tag{4.19}$$

A summation over the elements and use of (2.13) yields

$$\sum_{i=1}^{N} |\alpha_{ji}(0)|^2 \le C(u)h^{-2(p+1)}, \quad j = 1, 2. \tag{4.20}$$

A summation of (4.14) and use of (4.17), (4.18), (4.20), and the dominance of the exponential relative to any algebraic power of h yields (4.11a).

Following the reasoning used to obtain (4.14), we find

$$b_j^2(t) \le C[e^{-2r_j t}b_j^2(0) + \frac{|G_j(t)|^2}{r_j^2} + e^{-2r_j t}\frac{|G_j(0)|^2}{r_j^2} + e^{-2r_j(t-t_0)}\int_0^{t_0}\frac{|G_j'(\tau)|^2}{r_j^3}d\tau$$

$$+ \int_{t_0}^{t}\frac{|G_j'(\tau)|^2}{r_j^3}d\tau], \quad t \ge 0. \tag{4.21}$$

Once again, we must bound the various terms in (4.21). Thus, applying the Schwarz inequality to (4.3a) while using (4.6d) and (4.5), we obtain

$$\sum_{i=1}^{N}\frac{|G_{ji}(t)|^2}{r_{ji}^s} \le \sum_{i=1}^{N}\frac{C}{r_{ji}^s}\left\{\frac{\|v_j\|_{1,\Delta_i}}{\iint_{\Delta_i}\psi^2_{p+1,i}(x_j)\delta(x_{(j \bmod 2)+1})\,dx_1dx_2}\right\}^2(\|\partial_t e\|^2_{0,\Delta_i} + \|e\|^2_{1,\Delta_i})$$

$$\le Ch^{2(s-p-3)}(\|\partial_t e\|_0^2 + \|e\|_1^2], \quad j = 1, 2, \quad s \ge 0, 2, \quad t \ge 0. \tag{4.22}$$

The estimates (2.7b,c) and assumed bounds on e yield

$$\sum_{i=1}^{N}\frac{|G_{ji}(t)|^2}{r_{ji}^s} \le \begin{cases} C(u)h^{2(s-p-3)}, & \text{if } 0 \le t \le t_0 \\ C(u)h^{2(s-3)}, & \text{if } t_0 < t \end{cases}, \quad j = 1, 2, \quad s \ge 0. \tag{4.23}$$

Similarly,

$$\sum_{i=1}^{N}\frac{|G_{ji}'(t)|^2}{r_{ji}^3} \le \begin{cases} C(u)h^{-2p}, & \text{if } 0 \le t \le t_0 \\ C(u), & \text{if } t_0 < t \end{cases}, \quad j = 1, 2. \tag{4.24}$$

Likewise, using (4.6b) and (4.5), we obtain

$$\sum_{i=1}^{N} b_{ji}(0)^2 \le C\sum_{i=1}^{N}\left[\frac{\|v_j\|_{1,\Delta_i}}{\iint_{\Delta_i}\sigma(x_j)^2\delta(x_{(j \bmod 2)+1})\,dx_1dx_2}\right]^2 \|u^0(\cdot,0)-U(\cdot,0)\|^2_{1,\Delta_i} \le C(u)h^{-2(p+1)},$$

$$j = 1, 2. \tag{4.25}$$

A summation of (4.22) over the elements and subsequent use of (4.23-25) yields

$$\sum_{i=1}^{N} b_{ji}^2(t) \le C(u)h^{-2}, \quad t > t_0. \tag{4.26}$$

Differentiating (2.10b), and using (2.10d), (4.2c), and (4.5d) we readily obtain

$$\beta_j^2(t) = \frac{\|\partial_{x_j}\phi(\cdot,t)\|^2_{0,\Delta}}{\|\sigma(x_j)\|^2_{0,\Delta}} \le \frac{C}{h^2}\|u\|^2_{p+1,\Delta}, \quad j = 1, 2, \quad t \ge 0. \tag{4.27}$$

Combining (4.26) and (4.27)

$$\sum_{i=1}^{N}[b_{ji}^2(t)+\beta_{ji}^2(t)] \le \frac{C(u)}{h^2}, \quad t > t_0. \tag{4.28}$$

Applying the Schwarz inequality

$$\sum_{i=1}^{N}[\beta_{ji}^2(t)-b_{ji}^2(t)] \le C[\sum_{i=1}^{N}(\beta_{ji}(t)-b_{ji}(t))^2]^{1/2}[\sum_{i=1}^{N}(\beta_{ji}^2(t)+b_{ji}^2(t))]^{1/2} \tag{4.29}$$

while using (4.11a) and (4.28) leads to (4.11b). □

We are now in position to state and prove the main result of this section.

THEOREM 4.1. *Let $u \in H_0^1 \cap H^{p+2}$ and $U \in S_0^{N,p}$ be solutions of (2.2) and (2.3), respectively. If $p \ge 2$ is an even integer and there is a constant $C > 0$ such that $\|\partial_t^n e\|_1 \le C(u)$, $n = 0, 1$, then there exist constants $C > 0$ and $t_0 > 0$ such that*

$$\|e(\cdot,t)\|_1^2 = \|E(\cdot,t)\|_1^2 + \varepsilon, \quad t > t_0, \tag{4.30a}$$

where

$$\|E(\cdot,t)\|_1^2 = \sum_{i=1}^{N}\sum_{j=1}^{2} b_{ji}^2(t)\|\sigma(x_j)\|^2_{0,\Delta_i}, \quad |\varepsilon| \le Ch^{2p+1}. \tag{4.30b,c}$$

Proof. Consider the identity

$$\|e(\cdot,t)\|_1^2 = \sum_{i=1}^{N} \iint_{\Delta_i} (|\partial_{x_1} e|^2 + |\partial_{x_2} e|^2)\, dx_1 dx_2 + \|e\|_0^2 \tag{4.31}$$

and use (2.10b) and (2.15) to obtain

$$\|e\|_1^2 = \sum_{i=1}^{N} \iint_{\Delta_i} \sum_{j=1}^{2} [\beta_{ji}^2 \sigma^2(x_j) + |\partial_{x_j}\theta|^2 + 2\partial_{x_j}\phi\partial_{x_j}\theta]\, dx_1 dx_2 + \|e\|_0^2. \tag{4.32}$$

Adding and subtracting $b_{ji}^2\sigma^2(x_j)$, $j = 1, 2$, to the above integrand yields (4.30a,b) with

$$\varepsilon = \sum_{i=1}^{N} \sum_{j=1}^{2} \iint_{\Delta_i} [(\beta_{ji}^2 - b_{ji}^2)\sigma^2(x_j) + |\partial_{x_j}\theta|^2 + 2\partial_{x_j}\phi\partial_{x_j}\theta]\, dx_1 dx_2 + \|e\|_0^2. \tag{4.33}$$

Applying the Schwarz and triangular inequalities and using the estimates (2.13c,d), (4.11b) and (4.5d) yields (4.30c). □

4.2 The Elliptic error Estimate. As in §4.1, we further simplify the elliptic error estimation problem by neglecting the off-diagonal diffusion coefficients and the reaction term in the strain energy and by freezing the diagonal coefficients. With these approximations, $b_j(t)$, $j = 1, 2$, is determined from (4.4) as

$$b_j = \frac{g_\Delta(t,v_j)}{\bar{a}_{j,j} \iint_\Delta \sigma^2(x_j)\delta(x_{(j \bmod 2)+1})\, dx_1 dx_2}, \quad t > 0, \quad j = 1, 2. \tag{4.34}$$

Substituting (2.15) into (4.1a) while using (2.10b) yields

$$\bar{a}_{j,j}\beta_j(t) \iint_\Delta \sigma^2(x_j)\delta(x_{(j \bmod 2)+1})\, dx_1 dx_2 = g(t,v_j) - \hat{F}_j(t) \tag{4.35a}$$

where

$$\hat{F}_j(t) = \iint_\Delta [\sum_{k=1}^{2}\sum_{l=1}^{2} a_{k,l}\partial_{x_k} v_j \partial_{x_l}\theta + \sum_{k=1}^{2}\sum_{l=1}^{2} (a_{k,l} - \bar{a}_{k,l})\partial_{x_k} v_j \partial_{x_l}\phi + b v_j e + v_j \partial_t e]\, dx_1 dx_2, \quad j = 1, 2. \tag{4.35b}$$

Write (4.35a) in the form

$$\beta_j = \frac{g_\Delta(t,v_j) - \hat{F}_j}{\bar{a}_{j,j} \iint_\Delta \sigma^2(x_j)\delta(x_{(j \bmod 2)+1})\, dx_1 dx_2}, \quad j = 1, 2. \tag{4.36}$$

The analysis parallels that of §4.1 with a preliminary Lemma establishing differences between $\beta_j(t)$ and $b_j(t)$, $j = 1, 2$, and a subsequent Theorem containing the convergence result.

LEMMA 4.3. *Let $p \geq 2$ be an even integer, $u \in H_0^1 \cap H^{p+2}$, and $a_{k,k}(\mathbf{x}) > \alpha^0 > 0$, $\mathbf{x} \in \Omega$, $k = 1, 2$. Then, there are constants $C > 0$ such that*

$$\sum_{i=1}^{N} (\beta_{ji} - b_{ji})^2 \leq C(u), \quad \sum_{i=1}^{N} (\beta_{ji}^2 - b_{ji}^2) \leq \frac{C(u)}{h}, \quad j = 1, 2, \quad t > t_0. \tag{4.37a,b}$$

Proof. Subtracting (4.34) from (4.36) we obtain

$$\alpha_j(t) = -\frac{\hat{F}_j(t)}{\iint_{\Delta} \sigma^2(x_j)\delta(x_{(j \bmod 2)+1})\, dx_1 dx_2}, \quad t \geq 0, \quad j = 1, 2, \tag{4.38}$$

with $\alpha_j(t)$, $j = 1, 2$, given by (4.12). Applying the Schwarz and triangular inequalities to (4.38) while using (4.35b), the assumed smoothness of the diffusion coefficients, and the dominance of the H^1 norm relative to the L^2 norm yields

$$\alpha_j(t)^2 \leq C \|v_j\|_{1,\Delta}^2 \frac{[\|\theta\|_{1,\Delta}^2 + h^2\|\phi\|_{1,\Delta}^2 + \|e\|_{0,\Delta} + \|\partial_t e\|_{0,\Delta}^2]^2}{[\iint_{\Delta} \sigma^2(x_j)\delta(x_{(j \bmod 2)+1})\, dx_1 dx_2]^2}, \quad j = 1, 2. \tag{4.39}$$

Summing over the elements and using (4.5)

$$\sum_{i=1}^{N} \alpha_{j,i}(t)^2 \leq Ch^{-2(p+1)}[\|\Theta\|_1^2 + h^2\|\Phi\|_1^2 + \|e\|_0^2 + \|\partial_t e\|_0^2], \quad t \geq 0. \tag{4.40}$$

Using (2.7b) and (2.13c,d), we establish (4.37a).

Applying the same reasoning that was used to obtain (4.22-26), we obtain

$$b_j(t)^2 \leq Ch^{-2(p+1)}[\|\partial_t e\|_{0,\Delta}^2 + \|e\|_{1,\Delta}^2], \quad j = 1, 2, \quad t \geq 0. \tag{4.41}$$

Summing over the elements while using (2.7b,c)

$$\sum_{i=1}^{N} b_{ji}(t)^2 \leq \frac{C(u)}{h^2}, \quad t > t_0, \quad j = 1, 2. \tag{4.42}$$

Combining (4.27) and (4.42)

$$\sum_{i=1}^{N} [b_{ji}^2(t) + \beta_{ji}^2(t)] \le \frac{C(u)}{h^2}, \quad t > t_0. \tag{4.43}$$

Using (4.29) with (4.37a) and (4.43) establishes (4.37b). □

THEOREM 4.2. *Let* $u \in H_0^1 \cap H^{p+2}$ *and* $U \in S_0^{N,p}$ *be solutions of (2.2) and (2.3), respectively. If* $p \ge 2$ *is an even integer, then there exist constants* $C > 0$ *and* $t_0 > 0$ *such that*

$$\|e(\cdot,t)\|_1^2 = \|E(\cdot,t)\|_1^2 + \varepsilon, \quad t > t_0, \tag{4.44a}$$

where

$$\|E(\cdot,t)\|_1^2 = \sum_{i=1}^{N} \sum_{j=1}^{2} b_{ji}^2(t) \|\sigma(x_j)\|_{0,\Delta_i}^2, \quad |\varepsilon| \le Ch^{2p+1}. \tag{4.44b,c}$$

Proof. The proof is the same as that of Theorem 4.1. □

5. Examples. We present four examples to illustrate the performance of the error estimation procedures of §3 and §4 in situations where the theory applies and does not apply. Accuracy of the error estimate is measured by the global and local *effectivity indices*

$$\eta = \frac{\|E(\cdot,t)\|_1}{\|e(\cdot,t)\|_1}, \quad \eta_i = \frac{\|E(\cdot,t)\|_{1,\Delta_i}}{\|e(\cdot,t)\|_{1,\Delta_i}}, \quad i = 1, 2, ..., N, \tag{5.1}$$

respectively, which should converge to unity under mesh refinement. In all cases, even-order results are presented for the elliptic error estimation procedure. Results with the parabolic error estimation procedure are virtually identical.

Example 1. The theory applies to the linear heat conduction equation

$$\partial_t u - \Delta u = f(\mathbf{x},t), \quad \mathbf{x} \in (0,1)\times(0,1), \quad t > 0, \tag{5.2a}$$

with $f(\mathbf{x},t)$ and the initial and the Dirichlet boundary conditions specified so that the exact solution is

$$u(\mathbf{x},t) = cos(t)e^{-10[(x-½)^2 - (y-½)^2]}. \tag{5.2b}$$

We solved this problem on $0 < t \leq 0.5$ using uniform meshes having $N = 100$, 400, 900, and 1600 square elements and uniform orders $p = 1, 2, 3, 4$. Temporal integration was performed using the backward difference software system DASSL [13] with error tolerances of 10^{-6} for $p = 1, 2$ and 10^{-10} for $p = 3, 4$, which should minimize temporal discretization errors and enable us to concentrate on spatial errors. Finite element errors and effectivity indices at $t = 0.5$ appear in Table 1. Numbers in parenthesis indicate a power of ten.

Effectivity indices are in excess of 95% of ideal for all combinations of p and N. Convergence in h of the effectivity index to unity is apparent. Based on the limited data available in Table 1, converence in p seems plausible for even orders but not so for odd orders.

Example 2. Convection is not supported by the theory, but the error estimates should work as long as convection does not dominate diffusion. Thus, consider a linear convection-diffusion equation

$$\partial_t u - \Delta u + \nabla\cdot u = f(\mathbf{x},t), \quad \mathbf{x} \in (0,1)\times(0,1), \quad t > 0, \tag{5.3a}$$

with the data specified so that the exact solution is

$$u(\mathbf{x},t) = ½[1 - \tanh(10x_1 + 2x_2 - 10t - 2)]. \tag{5.3b}$$

We solved (5.3) using the parameters of Example 1. Finite element errors and effectivity indices at $t = 0.5$ appear in Table 2. As conjectured, the effectivity index appears to be approaching unity as N increases. Effectivity indices are above 80% of ideal for almost all computations. Performance of the even-order error estimates is better than that of the odd-order estimates. Again, the even-order indices suggest possible convergence in p.

Example 3. Although the present theory does not apply to nonlinear problems, we

TABLE 1
Errors and effectivity indices for Example 1 on N-element uniform meshes with piecewise bi-p polynomial approximations.

p	1		2		3		4	
N	$\|\|e\|\|_1/\|\|u\|\|_1$	η	$\|\|e\|\|_1/\|\|u\|\|_1$	η	$\|\|e\|\|_1/\|\|u\|\|_1$	η	$\|\|e\|\|_1/\|\|u\|\|_1$	η
100	0.151(0)	0.988	0.137(−1)	0.9961	0.987(−3)	0.948	0.587(−4)	0.9991
400	0.757(−1)	0.998	0.345(−2)	0.9990	0.124(−3)	0.983	0.369(−5)	0.9998
900	0.505(−1)	0.999	0.154(−2)	0.9996	0.369(−4)	0.992	0.731(−6)	0.9999
1600	0.379(−1)	0.999	0.864(−3)	0.9998	0.156(−4)	0.995	0.231(−6)	0.9999

TABLE 2
Errors and effectivity indices for Example 2 on N-element uniform meshes with piecewise bi-p polynomial approximations.

p	1		2		3		4	
N	$\|\|e\|\|_1/\|\|u\|\|_1$	η	$\|\|e\|\|_1/\|\|u\|\|_1$	η	$\|\|e\|\|_1/\|\|u\|\|_1$	η	$\|\|e\|\|_1/\|\|u\|\|_1$	η
100	0.239(0)	0.739	0.504(−1)	0.885	0.958(−2)	0.426	0.177(−2)	0.920
400	0.118(0)	0.928	0.127(−1)	0.970	0.125(−2)	0.754	0.118(−3)	0.979
900	0.785(−1)	0.968	0.569(−2)	0.987	0.377(−3)	0.880	0.238(−4)	0.991
1600	0.589(−1)	0.981	0.320(−2)	0.992	0.160(−3)	0.930	0.331(−4)	0.995

TABLE 3
Errors and effectivity indices for Example 3 on N-element uniform meshes with piecewise bi-p polynomial approximations.

p	1		2		3		4	
N	$\|\|e\|\|_1/\|\|u\|\|_1$	η	$\|\|e\|\|_1/\|\|u\|\|_1$	η	$\|\|e\|\|_1/\|\|u\|\|_1$	η	$\|\|e\|\|_1/\|\|u\|\|_1$	η
100	0.262(−1)	0.949	0.872(−3)	0.995	0.278(−4)	0.920	0.848(−6)	0.999
400	0.129(−1)	0.977	0.218(−3)	0.999	0.348(−5)	0.966	0.530(−7)	1.000
900	0.858(−2)	0.985	0.963(−4)	0.999	0.103(−5)	0.979	0.105(−7)	1.000
1600	0.643(−2)	0.989	0.544(−4)	1.000	0.436(−6)	0.979	0.331(−8)	1.000

expect good results when the nonlinearity is not strong and when the solution is smooth. Thus, consider the reaction-diffusion equation

$$\partial_t u - \tfrac{1}{2}\Delta u = qu^2(1-u), \quad \mathbf{x} \in (0,1)\times(0,1), \quad t > 0, \tag{5.4a}$$

with $q \geq 0$ and the data specified so that the exact solution is

$$u(\mathbf{x},t) = \frac{1}{1 + e^{\sqrt{q/2}(x_1 + x_2 - t\sqrt{q/2})}}. \tag{5.4b}$$

We selected $q = 20$ and solved (5.4) on $0 < t \leq 0.5$ using the parameters of Example 1. Temporal tolerances were selected as 10^{-10} for $p = 1, 2, 3$, 10^{-12} for $p = 4$ and the three coarser meshes, and 10^{-14} for $p = 4$ and the finest mesh.

Finite element errors and effectivity indices at $t = 0.5$ are presented in Table 3. The performance of the error estimation procedures is excellent, with effectivity indices in excess of 90% of ideal for all choices of N and p. As with the previous examples, convergence in h is apparent

Example 4. as a final example, consider a linear heat conduction equation of the form (5.2a) with the data specified so that the exact solution (expressed in polar coordinates) is

$$u(\mathbf{x},t) = u(r,\phi,t) = r^{\omega(t)}\sin\omega(t)\phi, \quad \omega(t) = (2/3) + (1/4)\sin t. \tag{5.5}$$

This solution behaves as $O(r^{\omega(t)})$ near the origin and this singular behavior will limit the rate of convergence in h. Unless the singularity is resolved by, e.g., grading the mesh, it will ''pollute'' the solution and error estimate globally. Our local error estiamtes fail to recognize such pollution errors and may be expected to give poor performance in their presence. Were the singularity resolved to the point where the pollution errors are small relative to the local errors, we would expect reasonable accuracy.

Let us begin by solving (5.2a, 5) on $0 < t \leq 0.3$ using the uniform meshes and polynomial degrees specified with Example 1. Temporal tolerances are 10^{-4}, 10^{-6}, 10^{-7}, and 10^{-10} for $p = 1, 2, 3, 4$, respectively. Errors and effectivity indices at $t = 0.3$ are shown in Table 4 for all combinations of N and p. Similar data at $t = 0.0, 0.1, 0.2$, and 0.3 for a 400-element uniform mesh with $p = 1, 2, 3, 4$ are shown in Table 5. Errors in the local H^1 norm and the difference between the local effectivity indices and unity at $t = 0.3$ for a 100-element mesh with $p = 4$ are shown in Figure 1.

Results in Tables 4 and 5 indicate that error estimates have little to do with exact errors. An examination of the upper portion of Figure 1 reveals that large errors near the

TABLE 4
Errors and effectivity indices for Example 4 on N-element uniform meshes with piecewise bi-p polynomial approximations.

p	1		2		3		4	
N	$\|\|e\|\|_1/\|\|u\|\|_1$	η	$\|\|e\|\|_1/\|\|u\|\|_1$	η	$\|\|e\|\|_1/\|\|u\|\|_1$	η	$\|\|e\|\|_1/\|\|u\|\|_1$	η
100	0.376(−1)	0.563	0.151(−1)	0.319	0.938(−2)	0.075	0.681(−2)	0.078
400	0.229(−1)	0.581	0.112(−1)	0.319	0.561(−2)	0.075	0.407(−2)	0.078
900	0.171(−1)	0.589	0.906(−2)	0.319	0.416(−2)	0.075	0.302(−2)	0.078
1600	0.138(−1)	0.593	0.768(−2)	0.319	0.336(−2)	0.075	0.244(−2)	0.078

TABLE 5
Errors and effectivity indices for Example 4 at $t = 0.0, 0.1, 0.2, 0.3$
on a 400-element uniform mesh with $p = 1, 2, 3, 4$.

p	1		2		3		4	
N	$\|\|e\|\|_1/\|\|u\|\|_1$	η	$\|\|e\|\|_1/\|\|u\|\|_1$	η	$\|\|e\|\|_1/\|\|u\|\|_1$	η	$\|\|e\|\|_1/\|\|u\|\|_1$	η
0.0	0.372(−1)	0.519	0.204(−1)	0.268	0.111(−1)	0.054	0.841(−2)	0.064
0.1	0.317(−1)	0.541	0.168(−1)	0.288	0.889(−2)	0.069	0.663(−2)	0.071
0.2	0.270(−1)	0.561	0.137(−1)	0.303	0.708(−2)	0.072	0.520(−2)	0.074
0.3	0.229(−1)	0.581	0.112(−1)	0.319	0.561(−2)	0.075	0.407(−2)	0.078

singularity pollute the entire domain and result in large deviations from unity of local effectivity indices everywhere [7]. As anticipated, the solution is converging as $O(h^{\omega(t)})$.

In order to improve the performance of the error estimations, we solve (5.2a, 5) on graded meshes obtained by refining the element of a uniform mesh that is closest to the origin. We do this by dividing the two element edges along the coordinate axis into the n segments

$$\xi_j = h(j/n)^{\zeta}, \quad j = 0, 1, \cdots, n, \quad \zeta > 0; \tag{5.6}$$

introducing a diagonal from from (ξ_1,ξ_1) to (h,h); and connecting line segments at the points (5.6) along the axes to similarly spaced points on the diagonal. This mesh, referred to as $N{:}n$, has N square and $2(n-1)$ trapezoidal elements. The mesh shown in the lower portion of Figure 1 is one uniform refinement of the 25:5 mesh. Error estimates can be constructed for these quadrilateral elements by introducing minor modifications to the

formulas developed here [1].

We solve (5.2a, 5) on $0 < t \leq 0.3$ using the meshes 25:5, 100:10, 225:15, and 400:20 with p ranging from 1 to 4. The grading parameter ζ was selected as 3/2 for $p = 1$ and $9p/4$ otherwise. Temporal tolerances are the same as the uniform-mesh case. Errors and effectivity indices at $t = 0.3$ are presented for all mesh and order combinations in Table 6. Similar data at $t = 0.0$, 0.1, 0.2, and 0.3 on the 132-element mesh appear in Table 7. Local errors and the difference between local effectivity indices and unity are shown in the lower portion of Figure 1.

The severe mesh grading has reduced errors on the element adjacent to the singularity. This has substantially reduced global pollution errors and improved the performance of the error estimation procedures. Global effectivity indices are within 12% of unity.

TABLE 6
Errors and effectivity indices for Example 4 on N-element graded meshes with piecewise bi-p polynomial approximations.

p	1		2		3		4	
N	$\|\|e\|\|_1/\|\|u\|\|_1$	η	$\|\|e\|\|_1/\|\|u\|\|_1$	η	$\|\|e\|\|_1/\|\|u\|\|_1$	η	$\|\|e\|\|_1/\|\|u\|\|_1$	η
132	0.181(−1)	0.999	0.118(−2)	0.941	0.369(−3)	3.431	0.234(−3)	0.879
472	0.112(−1)	1.004	0.468(−3)	1.016	0.453(−4)	1.279	0.682(−5)	1.039
1012	0.862(−2)	0.991	0.336(−3)	1.017	0.300(−4)	1.066	0.230(−5)	1.121
1752	0.704(−2)	0.993	0.271(−3)	1.017	0.241(−4)	0.989	0.177(−5)	1.080

TABLE 7
Errors and effectivity indices for Example 4 on a 472-element graded mesh with $p = 1, 2, 3, 4$.

p	1		2		3		4	
N	$\|\|e\|\|_1/\|\|u\|\|_1$	η	$\|\|e\|\|_1/\|\|u\|\|_1$	η	$\|\|e\|\|_1/\|\|u\|\|_1$	η	$\|\|e\|\|_1/\|\|u\|\|_1$	η
0.0	0.156(−1)	1.024	0.713(−3)	1.017	0.760(−4)	1.304	0.121(−4)	1.024
0.1	0.139(−1)	1.025	0.624(−3)	1.017	0.642(−4)	1.297	0.100(−4)	1.035
0.2	0.125(−1)	1.019	0.541(−3)	1.016	0.540(−4)	1.288	0.827(−5)	1.029
0.3	0.112(−1)	1.004	0.468(−3)	1.016	0.453(−4)	1.279	0.682(−5)	1.039

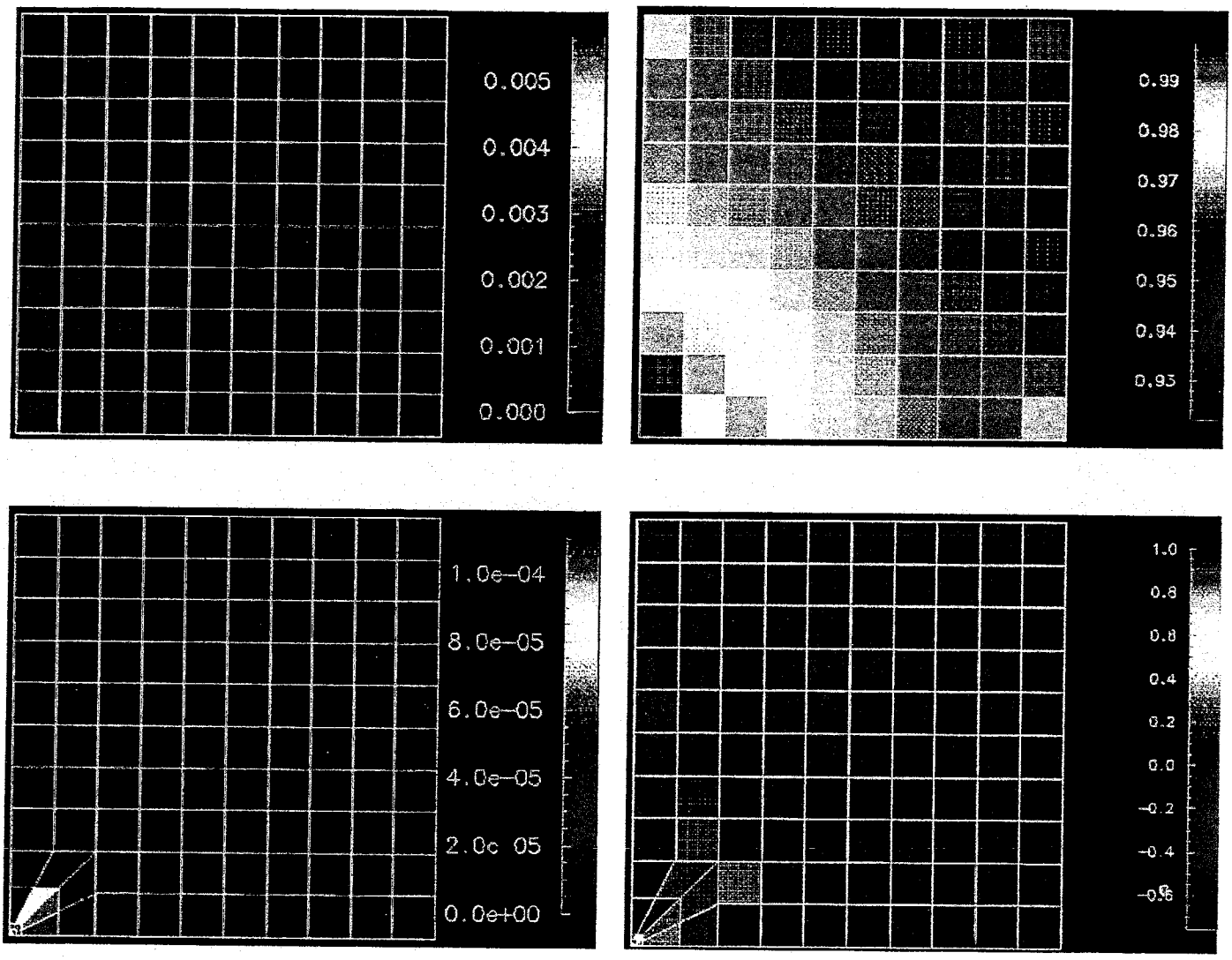

FIG. 1. *Local errors (upper-left) and the difference between the local effectivity indices and unity (upper-right) for Example 4 at* $t = 0.3$ *on a uniform 100-element mesh using piecewise bi-quartic polynomial approximations. Similar data for computations performed on a graded 5:5 mesh that has been uniformly refined are shown at the bottom.*

6. Discussion. We have developed simple a posteriori procedures for estimating spatial discretization errors of piecewise bi-p polynomial finite element solutions of linear parabolic partial differential equations. The theory developed for square-element meshes easily extends to rectangles. As earlier work [10, 18, 19] would suggest, the error estimation procedures divide into distinct classes for odd- and even-order approximations. Error estimates for each are asymptotically exact and involve only element level computations with, at most, nearest-neighbor communications.

The error estimates for even values of p perform better than that for odd p. Results indicate that asymptotic correctness under p-refinement is possible for even p. This is not the case for odd p where results deteriorate with increasing polynomial degree. Computational evidence further suggests that the error estimates are asymptotically correct under more general conditions than indicated by the present theory. Indeed, results of Example 4 indicate that the error estimates are asymptotically correct on graded quadrilateral-element meshes in the presence of singularities. Adjerid et al. [1] show that the error estimation procedures apply to finite element spaces other than piecewise bi-p polynomials. In particular, they apply to a class of piecewise hierarchical functions that have been modified by adding ''bubble functions'' to a standard hierarchical basis [14].

Extending the present theory to three-dimensional linear problems on hexahedral element-meshes would be straight forward. It would be more interesting and difficult to establish correctness of the error estimates on arbitrarily graded triangular- and tetrahedral-element meshes. Nonlinearity, strong reactions, convective influences, and singularities would be other important considerations.

REFERENCES

[1] S. Adjerid, B. Belguendouz, and J.E. Flaherty, *A posteriori finite element error estimation for diffusion problems,* SCOREC Rep. No. 9-1996, Sci. Comput. Res. Ctr., Rensselaer Polytechnic Institute, Troy, 1996.

[2] S. Adjerid and J.E. Flaherty, *A moving mesh finite element method with local refinement for parabolic partial differential equations,* Comp. Meths. Appl. Mech. and Engrg., 55 (1986), pp. 3-26.

[3] S. Adjerid, J.E. Flaherty, and Y.J. Wang, *A posteriori error estimation with finite element methods of lines for one-dimensional parabolic systems,* Numer. Math. 65 (1993), pp. 1-21.

[4] P.L. Baehmann, M.S. Shephard, and J.E. Flaherty, *Adaptive analysis for automated finite element modeling,* The Mathematics of Finite Elements and Applications VI, J.R. Whiteman, Ed., Academic Press, London, pp. 521-532, 1988.

[5] I. Babuška, J. Chandra, and J.E. Flaherty, Eds., Adaptive Computational Methods for Partial Differential Equations, SIAM, Philadelphia, 1983.

[6] I. Babuška and W.C. Reinboldt, *Reliable error estimation and mesh adaptation for the finite element method,* in Computational Methods in Nonlinear Mechanics, J.T. Oden, Ed., North-Holland, Amsterdam, 1980, pp. 67-108.

[7] I. Babuška, T. Strouboulis, A. Mathur, and C.S. Upadhyay, *Pollution-error in the h-version of the finite-element method and the local quality of a-posteriori error estimators,* Finite Elem. Anal. Des., 17 (1994), 273-321.

[8] I. Babuška, T. Strouboulis, and C.S. Upadhyay, *A model study of the quality of a-posteriori estimators for linear elliptic problems. Part Ia: Error estimation in the interior of patchwise uniform grids of triangles,* Tech. Note BN-1147, Inst. Physical Sci. and Tech., University of Maryland, College Park, 1993.

[9] I. Babuška, T. Strouboulis, C.S. Upadhyay, S.K. Gangaraj, and K. Copps, *Validation of a-posteriori error estimators by numerical approach,* Tech. Note BN-1151, Inst. Physical Sci. and Tech., University of Maryland, College Park, 1993.

[10] I. Babuška and D. Yu, *Asymptotically exact a-posteriori error estimator for biquadratic elements,* Finite Elem. Anal. Des., 3 (1987), 341-354.

[11] A.V. Ilin, B. Bagheri, R.W. Metcalfe, and L.R. Scott, *Error control and mesh optimization for high-order finite element approximation of incompressible viscous flow,* Comp. Meths. Appl. Mech. and Engrg., 1997, to appear.

[12] J.T. Oden and G.F. Carey, *Finite Elements: Mathematical Aspects, Vol. IV,* Prentice-Hall, Englewoods Cliffs, 1983.

[13] L.R. Petzold, *A description of DASSL: a differential/algebraic system solver,* Rep. Sand. 82-8637, Sandia National Laboratory, Livermore, 1982.

[14] B.A. Szabo and I. Babuška, *Introduction to Finite Element Analysis,* (J. Wiley and Sons, New York, 1991).

[15] V. Thomée, *Negative norm estimates and superconvergence in Galerkin Methods for parabolic problems,* Maths. Comp., 34 (1980), pp. 93-113.

[16] R. Verfürth, A review of a posteriori error estimation and adaptive mesh-refinement techniques, preprint, Institut für Angewandte mathematik, Universitat Zürich, Zürich, 1992.

[17] R. Wait and A.R. Mitchell, *Finite Element Analysis and Applications,* John Wiley and Sons, Chichester, 1985.

[18] D. Yu, *Asymptotically exact a-posteriori error estimator for elements of bi-even degree,* Mathematica Numerica Sinica, 13 (1991), pp. 89-101.

[19] D. Yu, *Asymptotically exact a-posteriori error estimator for elements of bi-odd degree,* Mathematica Numerica Sinica, 13 (1991), pp. 307-314.

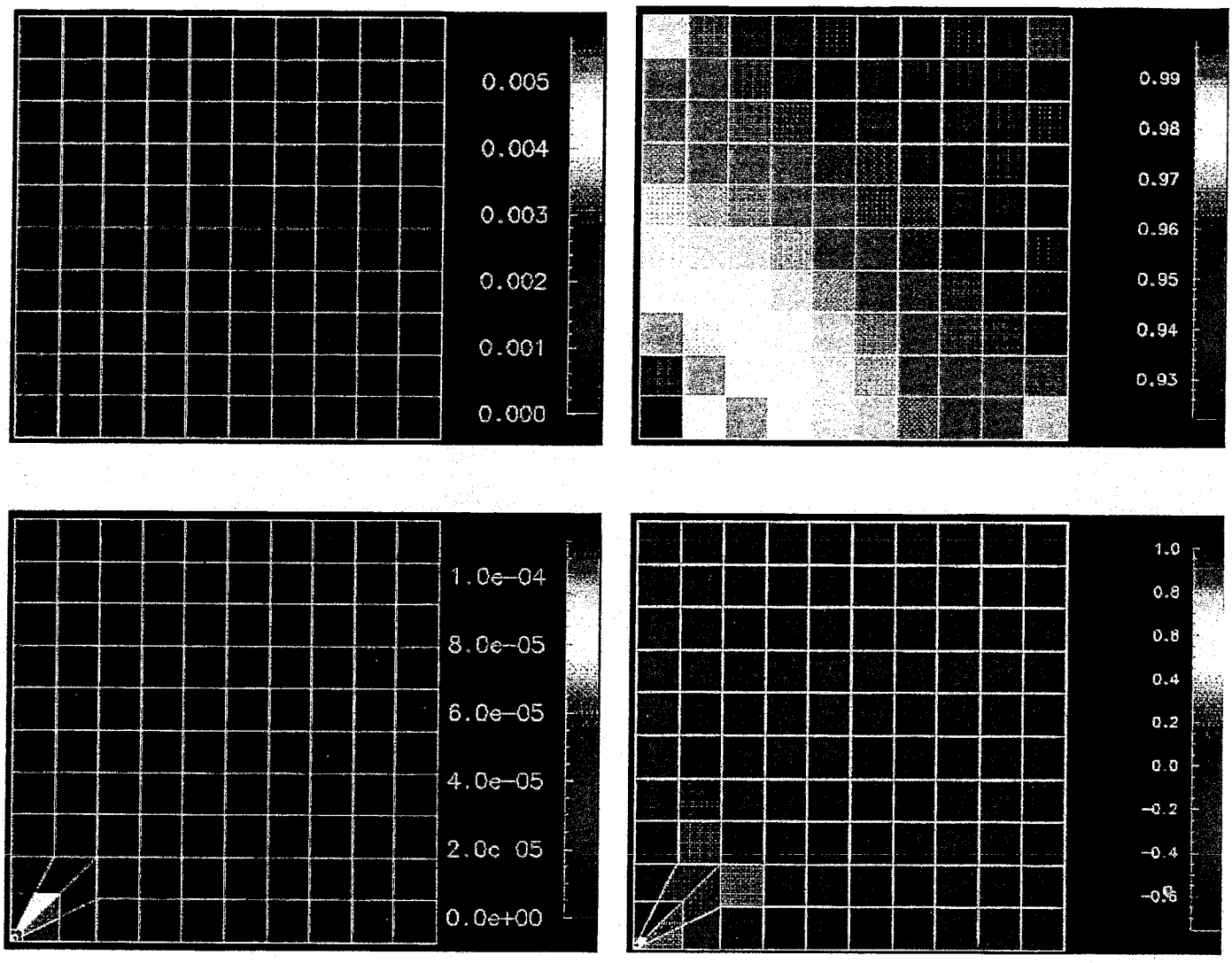

FIG. 1. *Local errors (upper-left) and the difference between the local effectivity indices and unity (upper-right) for Example 4 at* $t = 0.3$ *on a uniform 100-element mesh using piecewise bi-quartic polynomial approximations. Similar data for computations performed on a graded 5:5 mesh that has been uniformly refined are shown at the bottom.*

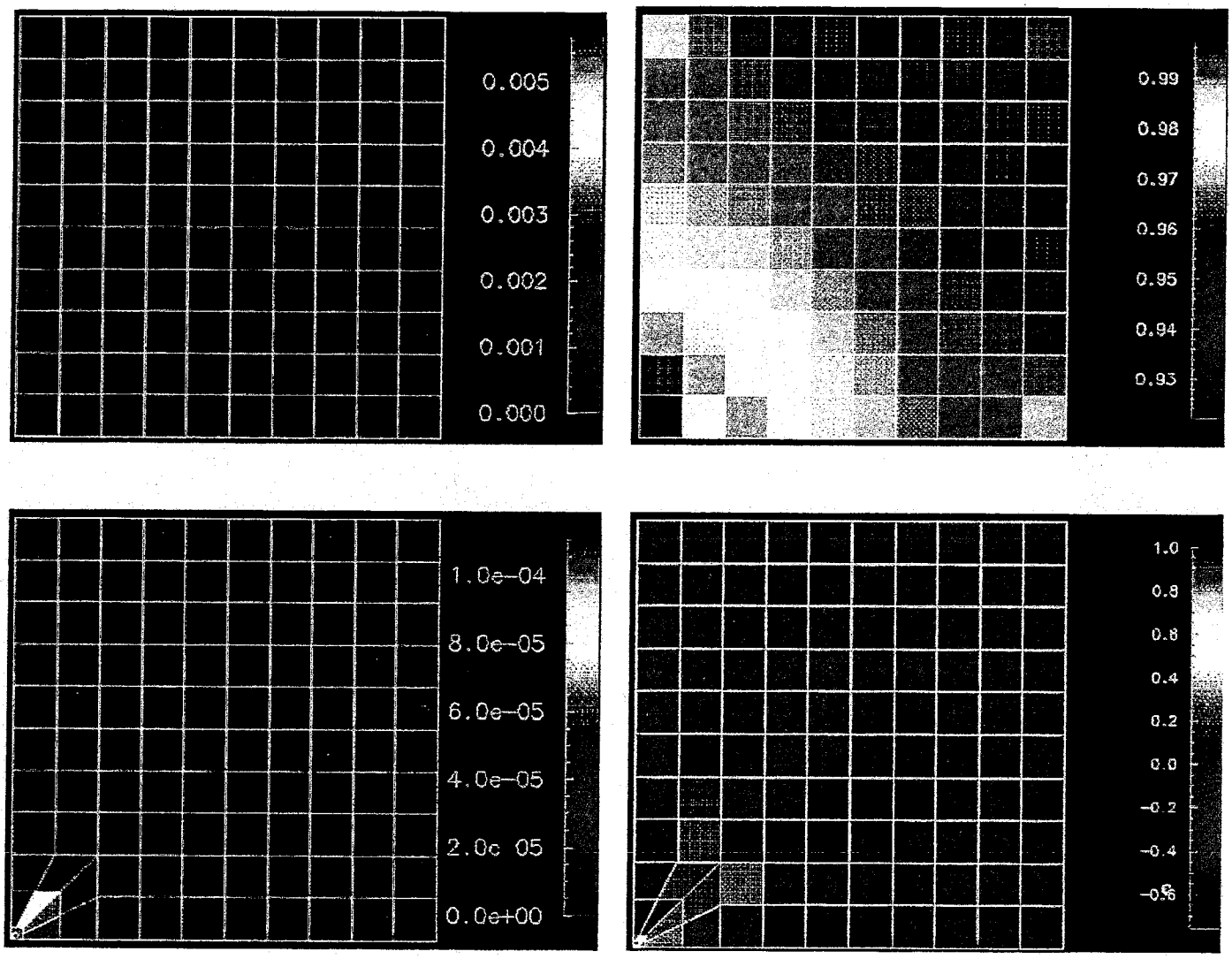

FIG. 1. *Local errors (upper-left) and the difference between the local effectivity indices and unity (upper-right) for Example 4 at* $t = 0.3$ *on a uniform 100-element mesh using piecewise bi-quartic polynomial approximations. Similar data for computations performed on a graded 5:5 mesh that has been uniformly refined are shown at the bottom.*

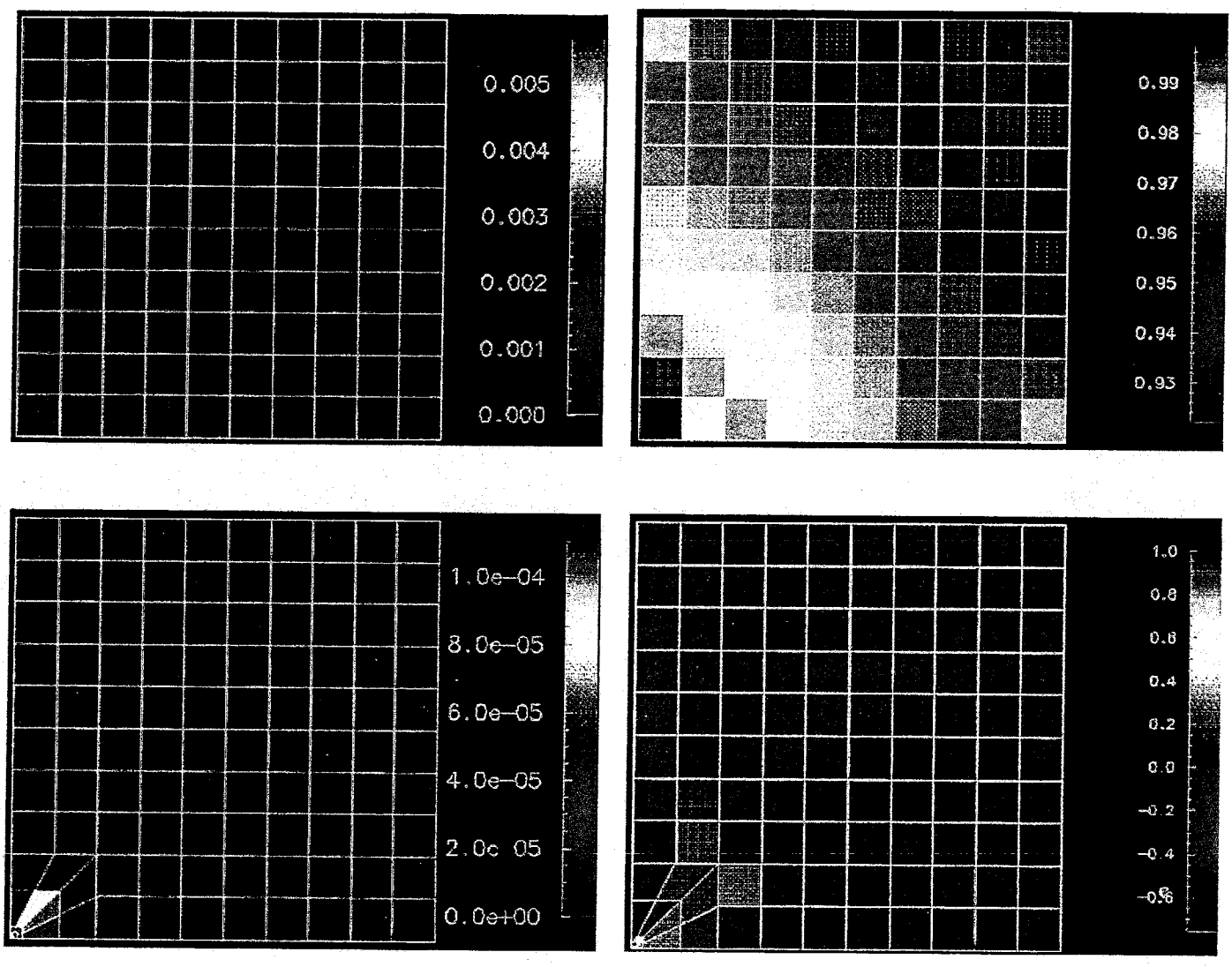

FIG. 1. *Local errors (upper-left) and the difference between the local effectivity indices and unity (upper-right) for Example 4 at* $t = 0.3$ *on a uniform 100-element mesh using piecewise bi-quartic polynomial approximations. Similar data for computations performed on a graded 5:5 mesh that has been uniformly refined are shown at the bottom.*

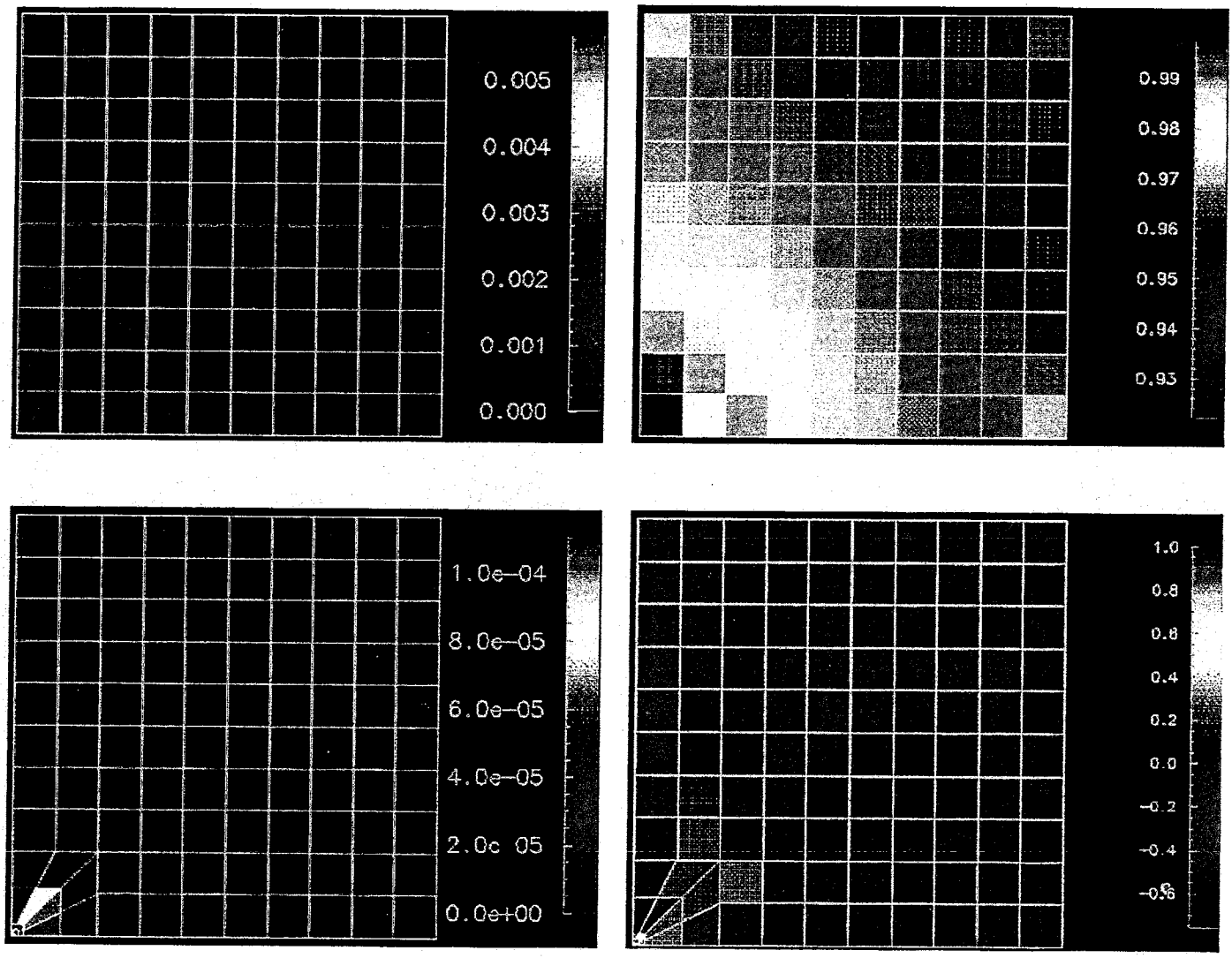

FIG. 1. *Local errors (upper-left) and the difference between the local effectivity indices and unity (upper-right) for Example 4 at* $t = 0.3$ *on a uniform 100-element mesh using piecewise bi-quartic polynomial approximations. Similar data for computations performed on a graded 5:5 mesh that has been uniformly refined are shown at the bottom.*

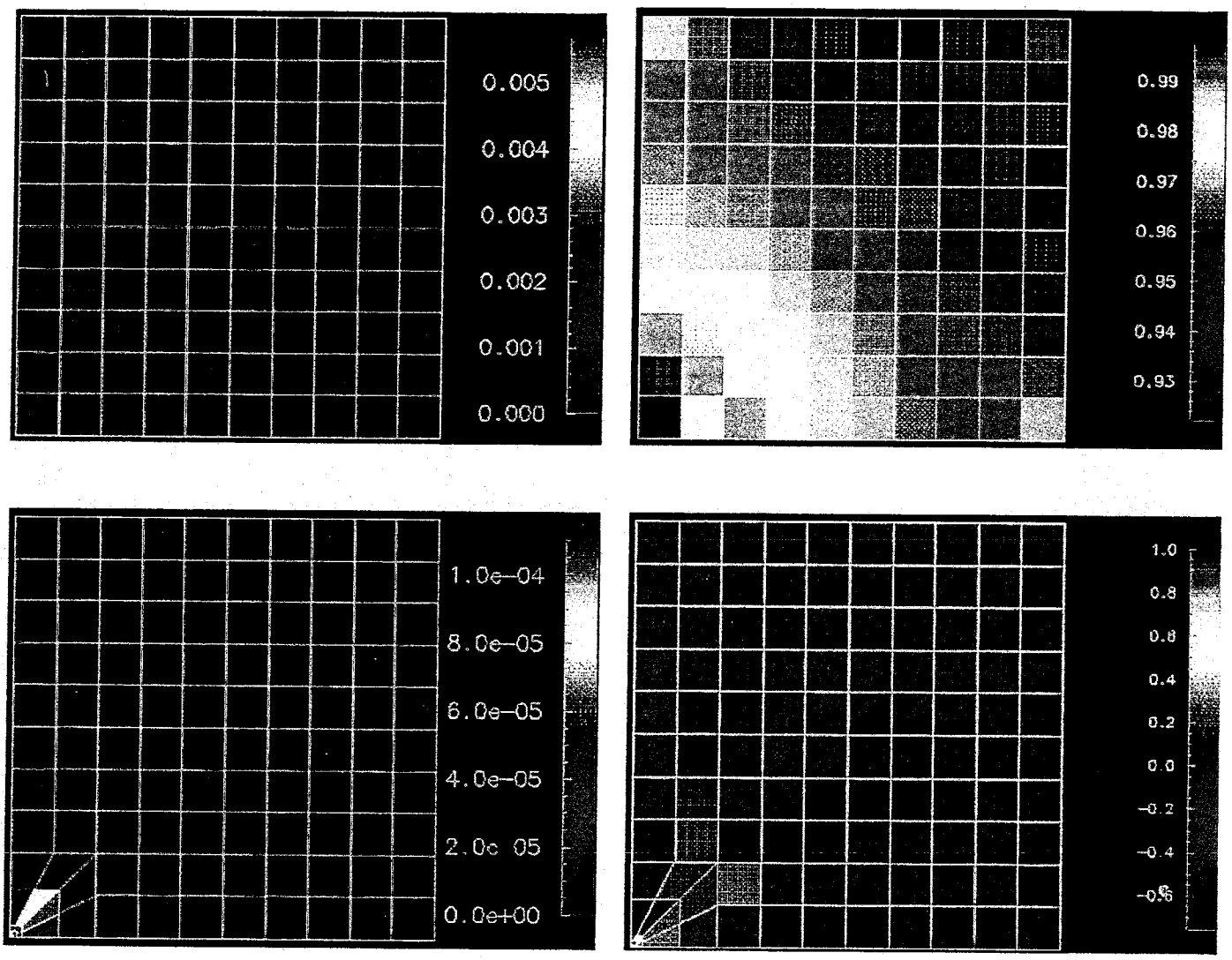

FIG. 1. *Local errors (upper-left) and the difference between the local effectivity indices and unity (upper-right) for Example 4 at* $t = 0.3$ *on a uniform 100-element mesh using piecewise bi-quartic polynomial approximations. Similar data for computations performed on a graded 5:5 mesh that has been uniformly refined are shown at the bottom.*

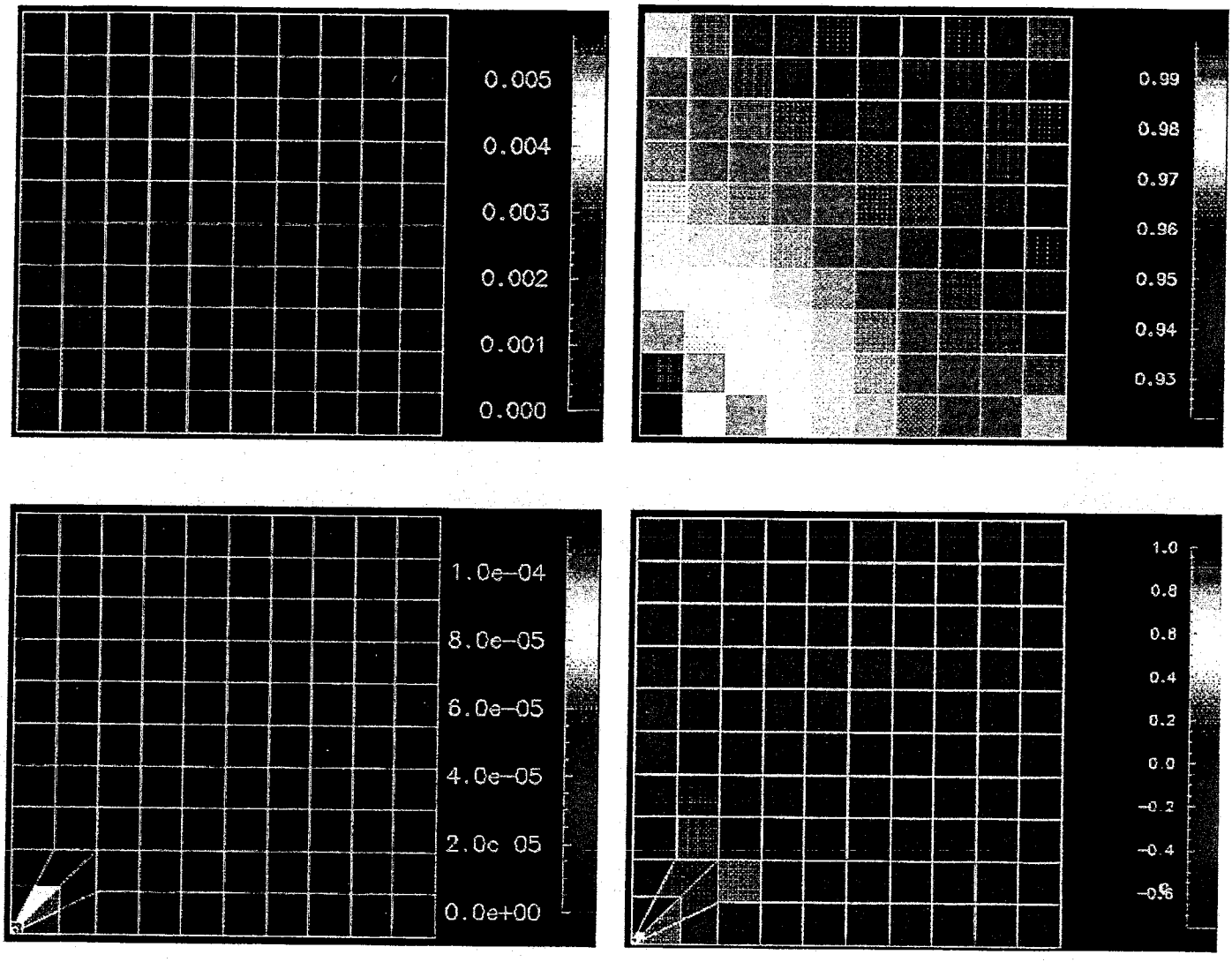

FIG. 1. *Local errors (upper-left) and the difference between the local effectivity indices and unity (upper-right) for Example 4 at* $t = 0.3$ *on a uniform 100-element mesh using piecewise bi-quartic polynomial approximations. Similar data for computations performed on a graded 5:5 mesh that has been uniformly refined are shown at the bottom.*

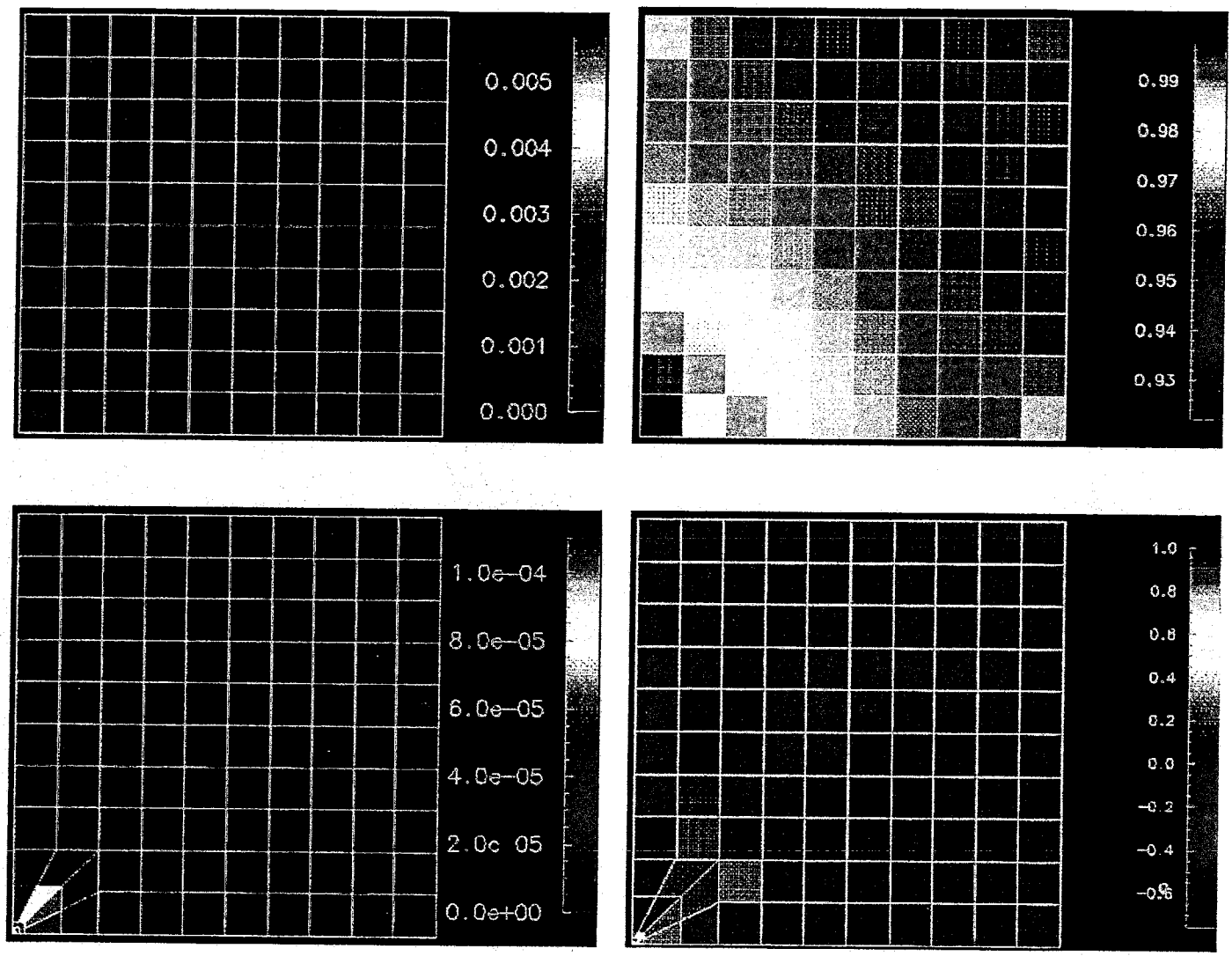

FIG. 1. *Local errors (upper-left) and the difference between the local effectivity indices and unity (upper-right) for Example 4 at* $t = 0.3$ *on a uniform 100-element mesh using piecewise bi-quartic polynomial approximations. Similar data for computations performed on a graded 5:5 mesh that has been uniformly refined are shown at the bottom.*

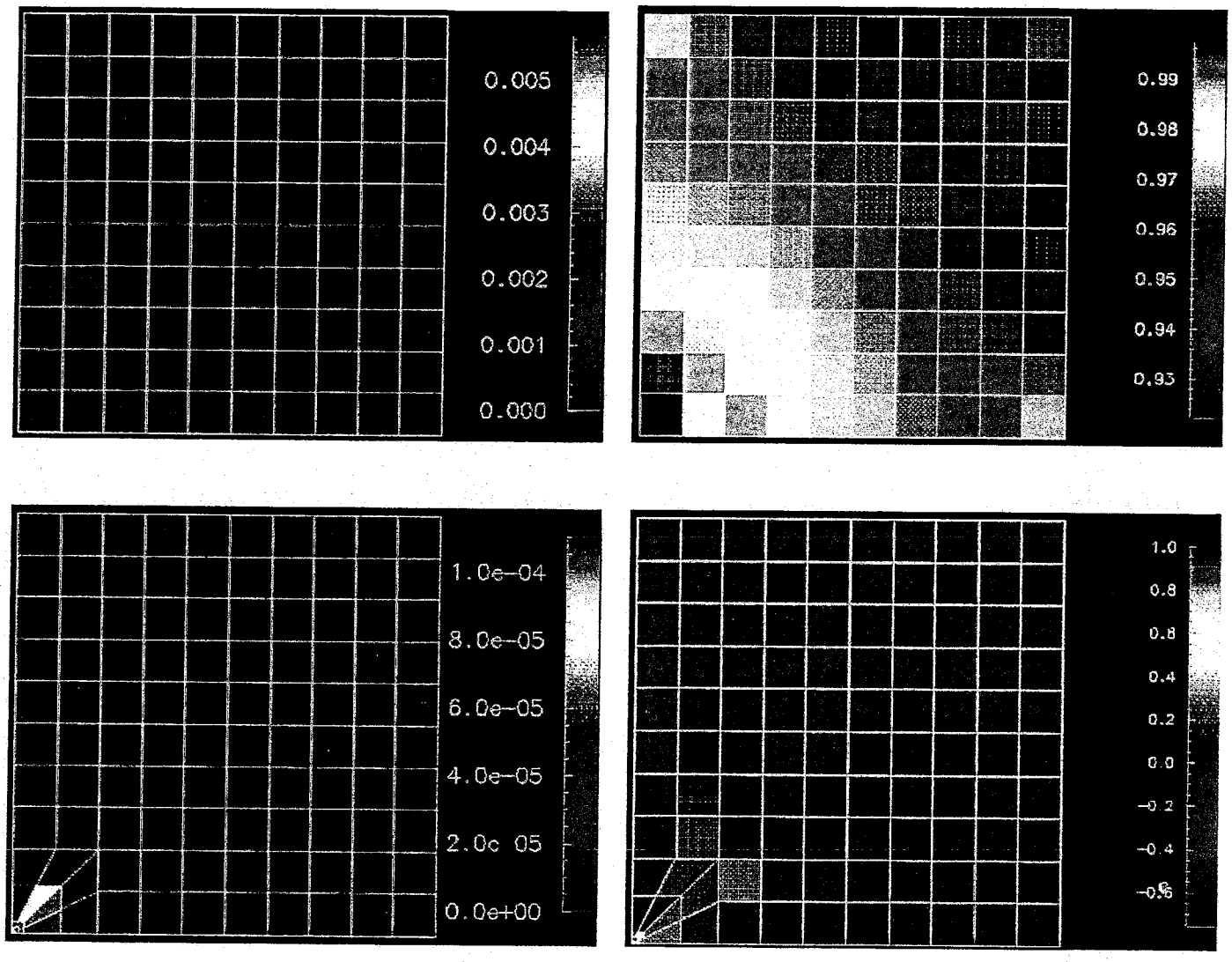

FIG. 1. *Local errors (upper-left) and the difference between the local effectivity indices and unity (upper-right) for Example 4 at $t = 0.3$ on a uniform 100-element mesh using piecewise bi-quartic polynomial approximations. Similar data for computations performed on a graded 5:5 mesh that has been uniformly refined are shown at the bottom.*

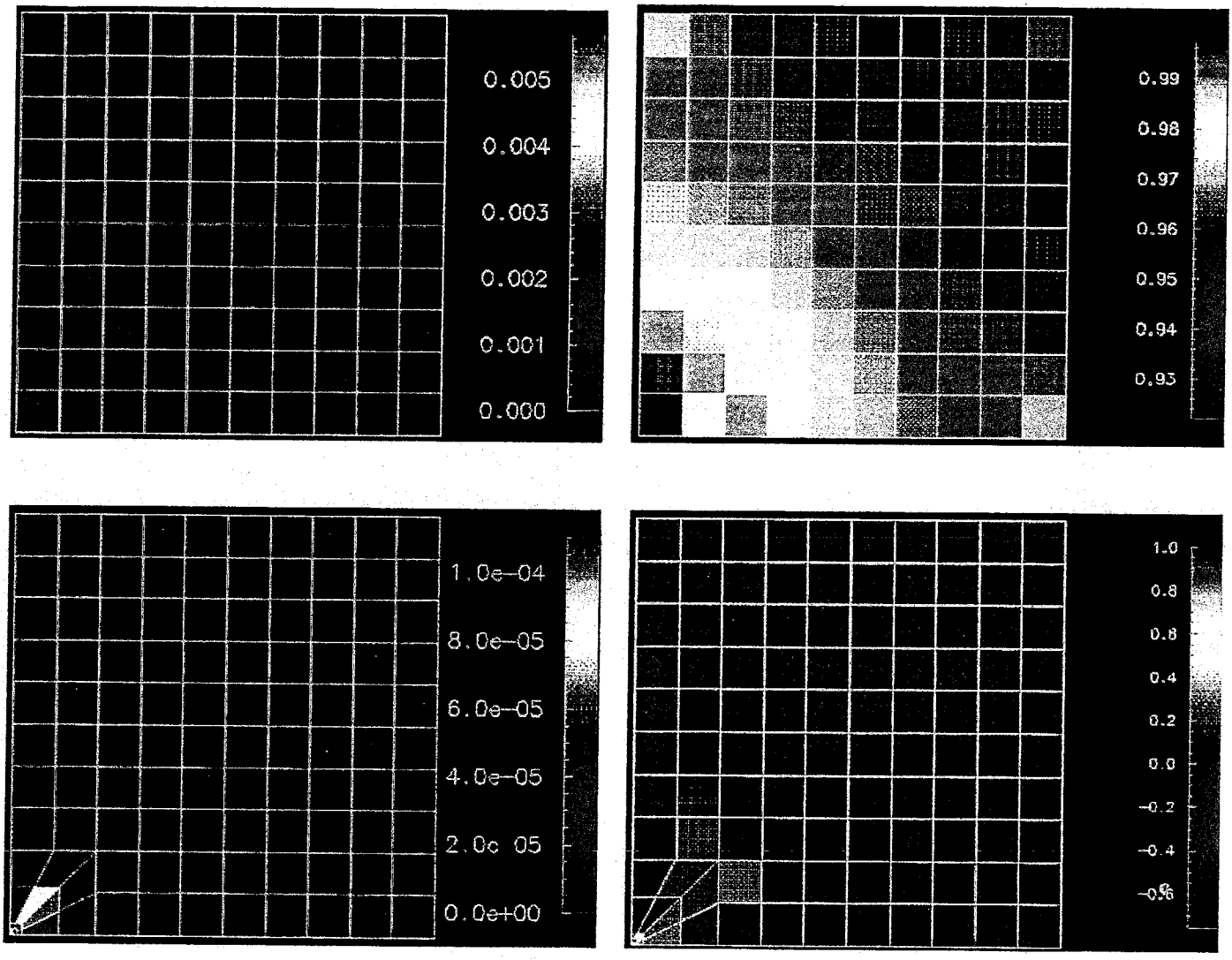

FIG. 1. *Local errors (upper-left) and the difference between the local effectivity indices and unity (upper-right) for Example 4 at* $t = 0.3$ *on a uniform 100-element mesh using piecewise bi-quartic polynomial approximations. Similar data for computations performed on a graded 5:5 mesh that has been uniformly refined are shown at the bottom.*

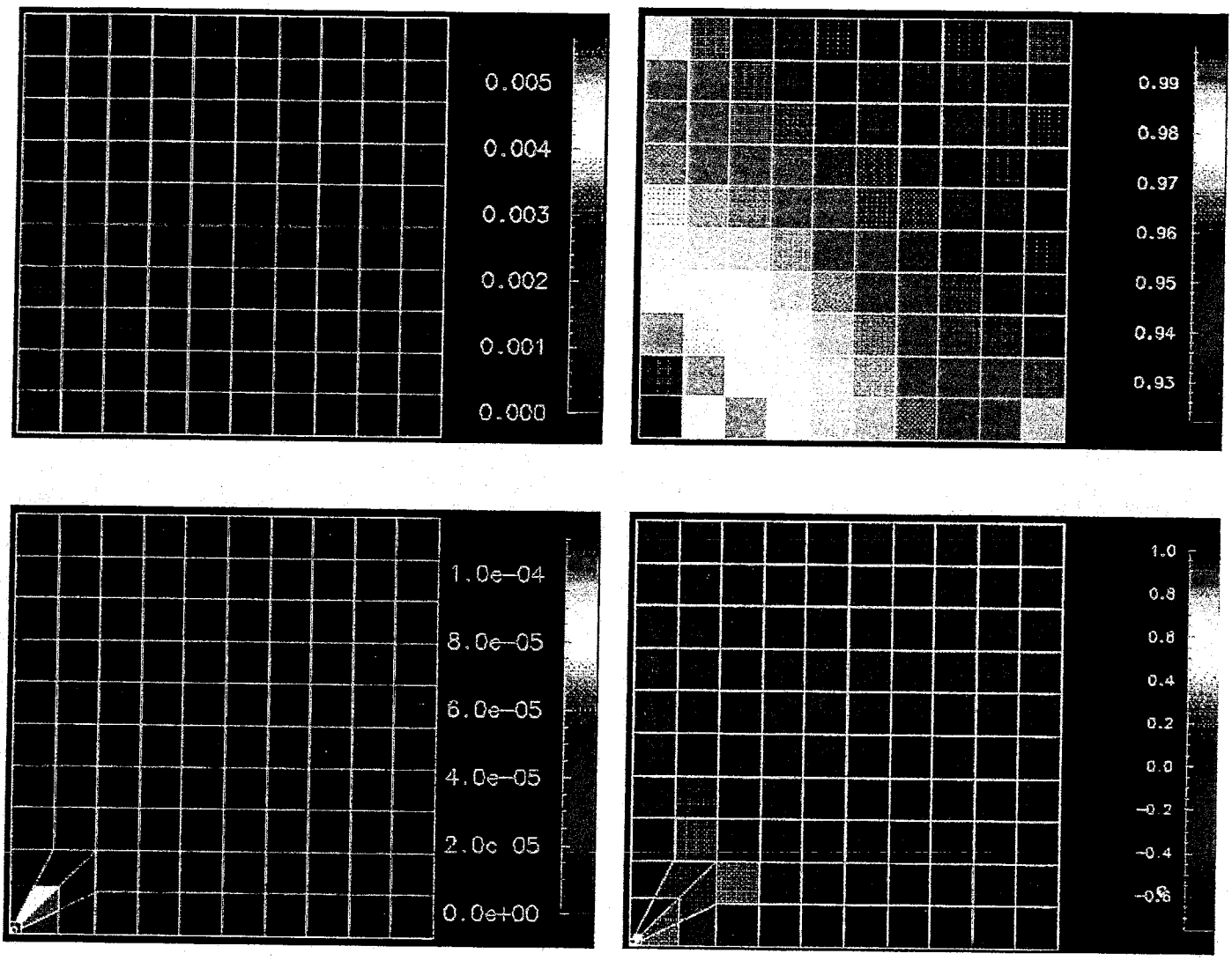

FIG. 1. *Local errors (upper-left) and the difference between the local effectivity indices and unity (upper-right) for Example 4 at* $t = 0.3$ *on a uniform 100-element mesh using piecewise bi-quartic polynomial approximations. Similar data for computations performed on a graded 5:5 mesh that has been uniformly refined are shown at the bottom.*

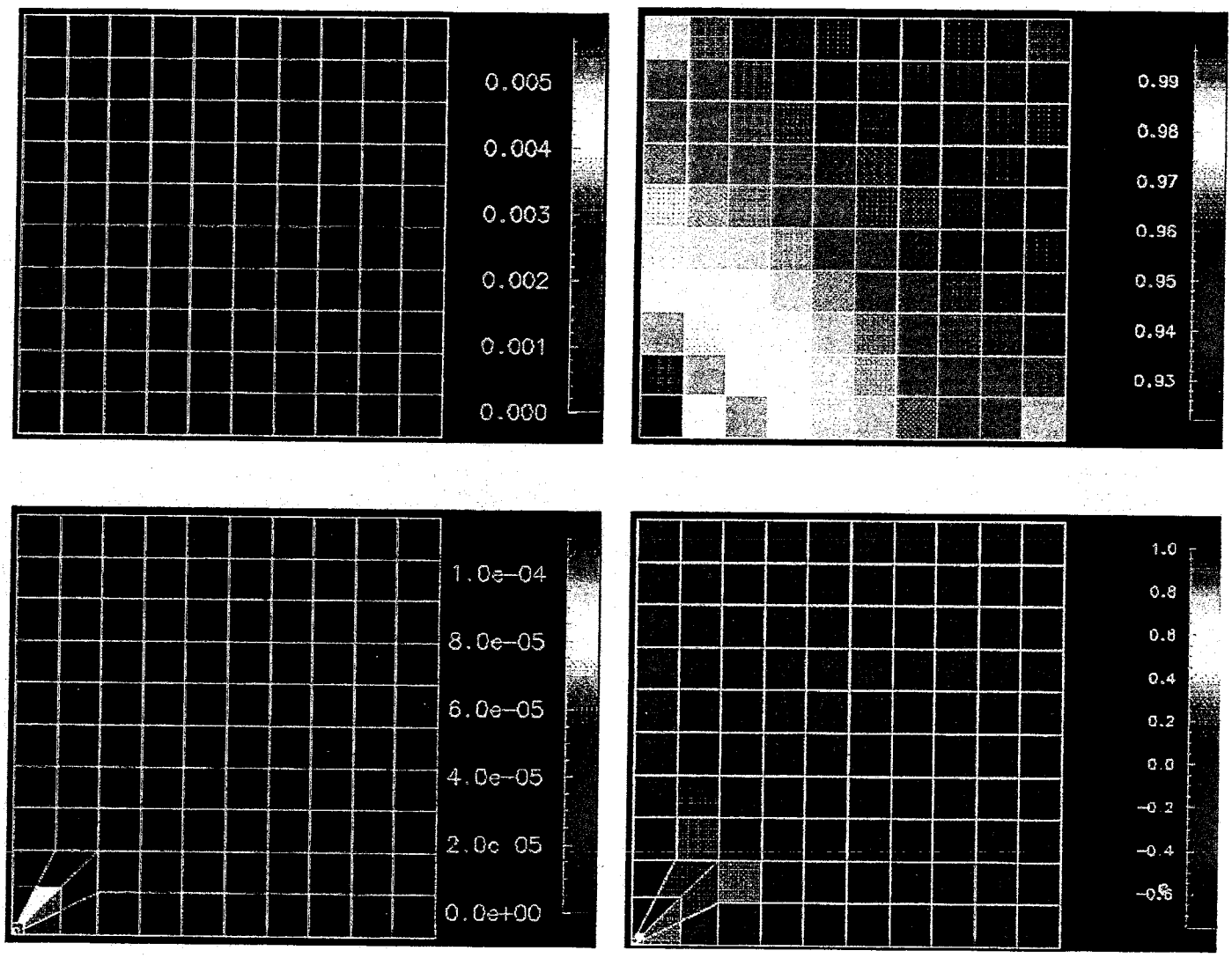

FIG. 1. *Local errors (upper-left) and the difference between the local effectivity indices and unity (upper-right) for Example 4 at* $t = 0.3$ *on a uniform 100-element mesh using piecewise bi-quartic polynomial approximations. Similar data for computations performed on a graded 5:5 mesh that has been uniformly refined are shown at the bottom.*

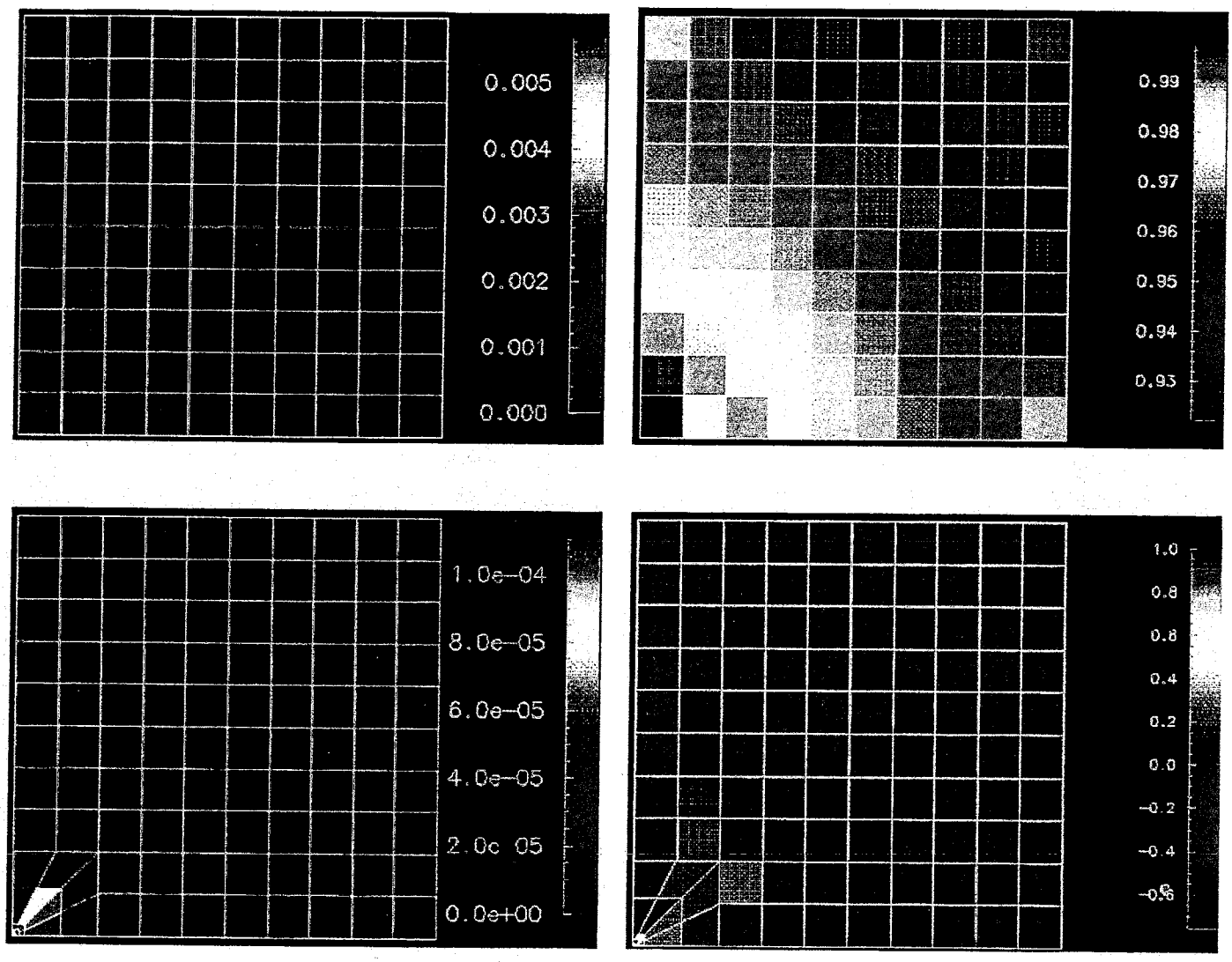

FIG. 1. *Local errors (upper-left) and the difference between the local effectivity indices and unity (upper-right) for Example 4 at* $t = 0.3$ *on a uniform 100-element mesh using piecewise bi-quartic polynomial approximations. Similar data for computations performed on a graded 5:5 mesh that has been uniformly refined are shown at the bottom.*

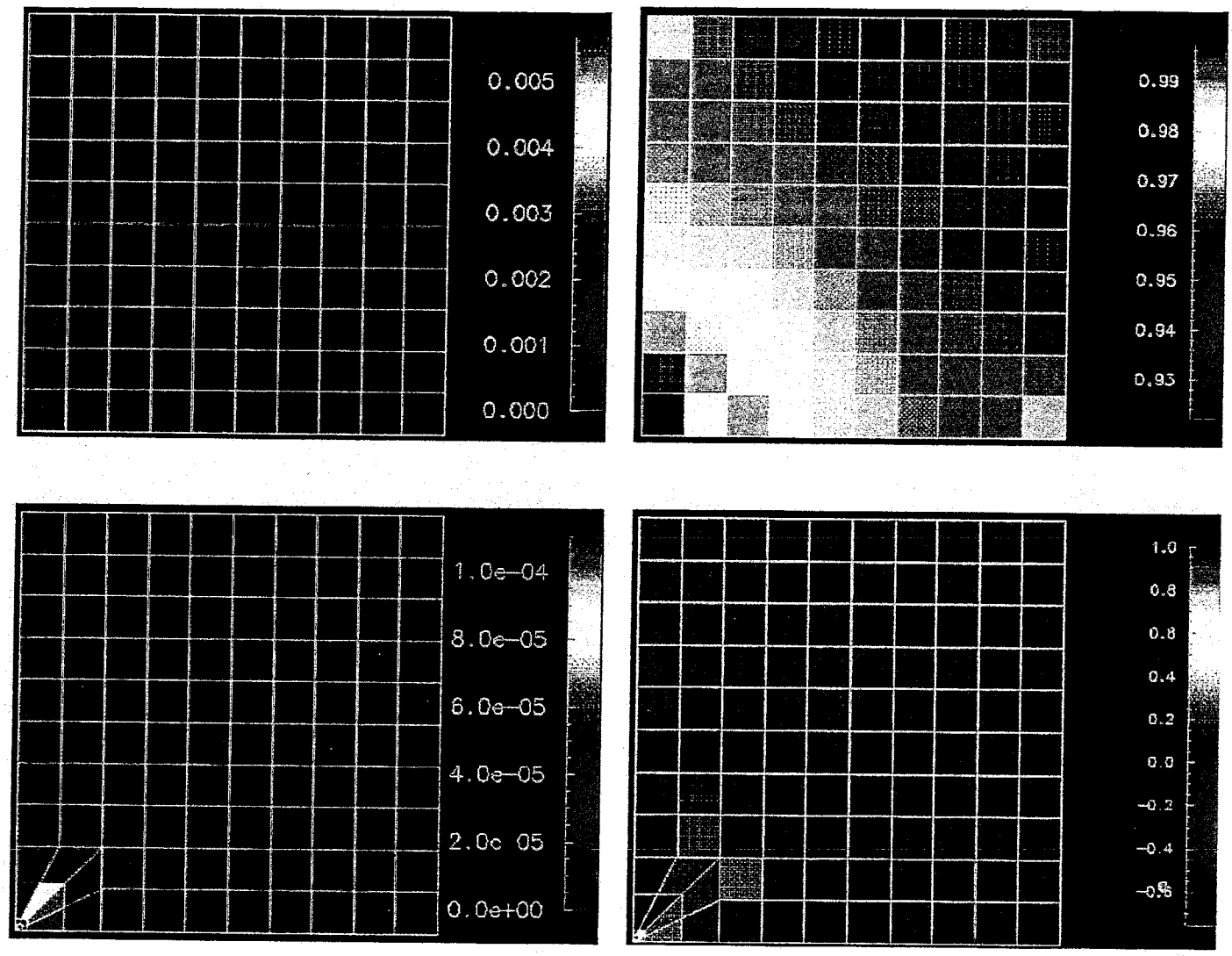

FIG. 1. *Local errors (upper-left) and the difference between the local effectivity indices and unity (upper-right) for Example 4 at* $t = 0.3$ *on a uniform 100-element mesh using piecewise bi-quartic polynomial approximations. Similar data for computations performed on a graded 5:5 mesh that has been uniformly refined are shown at the bottom.*